Report IDM Ref. No.	**EFDA_D_2QH7QK**	**Version:**

Technical Note / Report

Subtask ENS-6.1.4.0-T008-03

Design Status of the MuVacAS Experimental Setup 2022

	Technical Report
	Technical Note
	Other **Specify:**

		Document Id.	ENS-6.1.4.0-T008-03
Work Package:	**WPENS**	**Issue Date**	15-03-22

Document/Report Authors (refer to first page of actual report/document for a complete list)	
Author(s):	A. Sabogal, C. Torregrosa
RU:	*UGR*

Links to other files (CATIA CAD Files, Interface database,…)	
Title:	n/a
URL:	n/a

IDM Report Review & Approval	
IDM role	**Name(s)**
Author and co-author(s):	A. Sabogal, C. Torregrosa
Reviewer Task Owner	
Reviewer(s) Technical Issues:	P. Cara, A. Podadera, M. Ferreira
Approver:	A. Ibarra

Executive Summary

This report presents an overview of the technical design of the MuVacAS Experimental Setup, which is designed to recreate vacuum related accidental scenarios in IFMIF-DONES and to evaluate the performance of safety credited components to mitigate them. The report provides a description of the main systems of the setup and preliminary measurements achieved during first prototyping phases. The construction and assembly of the integral setup in the University of Granada is expected by the end of 2023, with the experimental campaigns starting in 2024.

Comments (shortcomings, deviations, etc.)

[Please indicate shortly here (if any) – details to be provided in document]

Record of modifications

Version	Date	Modification
V1.0	20/01/2023	

Table of Contents

List of Tables

List of Figures

List of Abbreviations

A list of general abbreviations of WPENS work package is given here: <u>(EFDA_D_2P9YDN v1.0)</u>

Abbreviation	Definition
CVVC	Control Volume Vacuum Chamber
CFD	Computational fluid dynamics
DAQ	Data acquisition
FIV	Fast Isolation Valve
FSIV	Fast Safety Isolation Valves
HEBT	High Energy Beam Transport
MFC	Mass Flow Controller
PU	Pumping Unit
QDS	Quick Disconnection System
RAS	Referent Accident Scenarios
RGA	Residual Gas Analyser
RIR	Radiation Isolation Room
TIR	Target Interface Room
TMP	Turbo-Molecular Pump
TVC	Target Vacuum Chamber
SIC	Safety Important Class
STP	Shock Tube Problem
VS	Vacuum System

1. Introduction

The MuVacAS (Multipurpose Vacuum Accident Scenarios) Setup has been conceived to experimentally recreate vacuum related accidental scenarios in IFMIF-DONES and to evaluate the performance of safety credited components to mitigate them. According to the events analysed in the Safety Analysis Report (SAR) [1], there are postulated three Reference Accident Scenarios (RAS) related to such vacuum loss in the beam line and target chamber. In particular:

RAS#5- LS3-3 Loss of vacuum in Target Vacuum Chamber.
RAS#12- AS3-1 Cooling water ingress in the accelerator beam duct.
RAS#13- AS3-2 Loss of vacuum in beam duct and air ingress.

In this context, the main objective of the MuVacAS setup is to recreate these RAS and study in detail (both numerically and experimentally) the involved propagation times of gas/liquid, transported mases in such events, and the efficacy of the Fast Safety Isolation Valves (FSIVs) as main mitigation mechanism, (also know as just Fast Isolation Valve, FIVs).

The previous technical report EFDA_D_2PE6K4 [2] presents a more detailed explanation of the MuVacAS justification, its objectives, conceptual design, and a preliminary literature review of past studies related to its scientific and technical aspects.

The current document is a continuation of the report [2], showing the progresses achieved during 2022, mainly focused on the detailed design of MuVacAS setup and preliminary experimental results obtained. It also provides a more consolidated literature review and some preliminary results of CFD simulations of a sudden gas inrush in a vacuum chamber.

In summary, the main objectives of the MuVacAS experiment can be classified in three types:

I. To recreate the vacuum loss RAS and study in detail the involved propagation times of gas/liquid and transported masses in such events. This includes controlled injections of water/gas to recreate potential leaks along the vacuum line as well as scenarios involving a sudden gas inrush, such as the TVC backplate rupture or a beam line seizure. In addition, modelling tools will be crosschecked and benchmarked with experimental data.

II. To validate the performance and efficacy of fast isolation valves and other mitigation measures in views to the future IFMIF-DONES licensing. This includes verifying closing times and pressure thresholds, optimizing the fast valve and measurement gauge positions, and serving as a test bench for the safety control architecture of the FSIVs and its reliability assessment for their SIC-1 classification.

III. Other complementary objectives of the setup include the design and testing of the differential pressure system along the HEBT and TVC through regulated injection of Ar in the target chamber, prototyping activities for vacuum components in the HEBT such as aluminium

chambers, flanges, pumping and measurement systems, and integration of remote handling QDS for the elements in the TIR and TVC-HEBT connection.

2. Literature Review

In the previous report EFDA_D_2PE6K4 [2] an extensive literature search was made based on three main topics: (i) investigations on sudden air inrushes in high vacuum systems, (ii) leaks of water inside vacuum, and (ii) applied cases in other facilities where FIVs (not necessarily Safety credited) were used as a mitigation mechanism of these events. In this section, we provide a compilation of the state-of-the-art, focusing on these references, the characteristics of their experimental setups and their most relevant results. These aspects are considered in the design of the MuVacAS experimental setup and future testing campaigns. At the end of the section, we present other important studies for which no publications are found so far.

2.1 Gas Inrushes and Injections in Vacuum Chambers
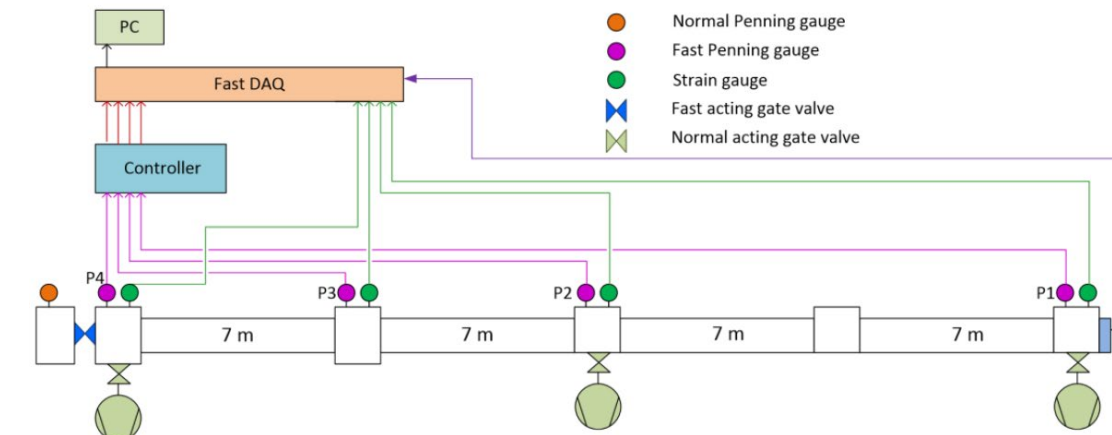
This section presents a summary the most relevant theoretical and experimental research studies found so far regarding sudden gas inrushes and controlled injections in vacuum.

Table 1 provides information about their objectives, experimental setup and some results. A timeline sketch with this biography is also provided in annex 1.

Table 1. Experimental test of sudden air inrush

Research	Objectives	Setup	Results
H. Bertz, 1979, [3] *Experimental test of sudden inrush of air and He.*	To test the design of acoustic delay systems for protection of synchrotrons lines.	• Inrush Mechanism: Knife, breaking foil window • FIV = DN 63 VAT • Line Length = 15 m • $P_{o\ vacuum}$ = from 10^{-6} to 10^{-3} mbar • Line diameter = 63 mm	• Fast Valve closing time = 19 ms (DN63) • Measured front propagation velocity: 1100 m/s for air 2000 m/s for He • Front Propagation Velocity is dependent to vacuum the initial vacuum pressure. • Well-dimensioned delay lines can effectively slowdown the propagation fronts.
W. Peatman, 1980, [4] *Experimental tests of sudden inrush.*	Similar experiments in DESY.	• Inrush Mechanism: pendulum and breaking foil window • Line Length = 8 m • $P_{o\ vacuum}$ = from 10^{-6} to 10^{-5} mbar • Line diameter = From 63 mm to 150 mm • No FIV was used	• Measured front propagation velocity: From 50 to 1000 m/s for air • Some hints that indicate that the shock wave velocity may be independent of pipe size are reported (not fully validated).

| T. Takiya, 1999, [5] *Experimental test and modelling of pressure wave propagation.* | Includes both theoretical estimations (unsteady tube-flow model) and experimental results | • Inrush Mechanism: needle breaking foil window.
• Line Length = 5 m
• $P_{o\ vacuum}$ = from 1.3 to 133 mbar
• Line diameter = 37 mm
• Entrance window diameter = 26 mm
• No FIV was used | • Measured front propagation velocity: 714 m/s in air (10% slower than theoretical prediction).
• Theoretically predicted front propagation speed:
• From 30 m/s to 2200 m/s depending on initial vacuum pressure and geometry d_{inlet}/d_{line} ratio. |
| M. Ady et al. CERN, Vacuum group Experiments performed in 2013-2014 [6] [7] | Experimental campaigns for assessing the protection system of the cryomodules in the HIE-ISOLDE line against air-inrush from downstream experimental stations. | • Inrush Mechanism: Pendulum breaking foil window.
• Line Length = 28 m
• $P_{o\ vacuum}$ = from 10^{-7} to $2 \cdot 10^{-6}$ mbar
• Line diameter = 80 mm
• FIV DN40 from VAT
• Pressure gauges: IKR070 Pfeiffer, acquiring at 19.2 kHz by at QuantumX MX840A HBM analogue-digital converter. | • Measured front propagation velocity:
• From 100 up to 800 m/s
• CFD simulations predicted front propagation speed of 620 m/s for $P_{o\ vacuum}$ = 10 mbar and a d_{inlet}/d_{line} = 0.125
• Highlighted potential issues with leak rates in the isolation valves |

2.2 Previous Studies of Water Inrush in Vacuum

A summary of two previous works related with studies of water inrush in vacuum is presented in the Table 2.

Table 2. Experimental studies of water inlet to vacuum chambers.

Research	Objectives	Setup	Results

M. Otawa, 1995 [8]	Studies focus on the eventual impingement of a water jet onto the plasma-facing wall and water evaporation on the event of ingress into a tokamak vacuum system.	• Injection of water jet to simulate different small breaks of the coolant pipes. • Nozzle diameters: 0.5, 1, 2 and 5 mm. • Mass flow rates: from 1.3 g/s to 500 g/s. • $P_{o\ vacuum}$ = 0.3 mbar	• Water freezes and blocks entrance channel when the nozzle using a 0.5 mm diameter and flow rate less than 2.4 g/s.

Size of vacuum enclosure (length, width, depth)	0.5, 0.3, 0.3 m
Enclosure pressures	$30 - 1.01 \times 10^5$ Pa
Enclosure wall temperatures	Atmospheric temperature (7-20 °C)
Size of hot plate (width, height, thickness)	0.12, 0.12, 0.02 m
Plate temperatures (wall superheats)	To 350 °C (to 300 K)
Water injection pressures	0.1-0.6 MPa
Water mass flow rates	$1.3 \times 10^{-3} - 0.50$ kg s^{-1}
Water temperatures	Atmospheric temperature (7-20 °C)
Diameters of injection nozzles	0.5, 1, 2, 5 mm

N. Garceau, 2019 [9]	Studies of transfer processes (heat and mass) involved in a sudden catastrophic loss of vacuum of a cryogenic system	• P vacuum = 10^{-6} Pa • Copper tube: diameter of 2.8 cm. • Solenoide valve simulate vacuum break with 25 ms opening time.	Propagation gas at 10 m/s due to the gas condensation to the tube wall.

2.3 Additional works about the use of FIVs and Gate Valves in other Facilities

One of the main MuVacAS objectives is to find the suitable architecture to reach the required reliability of the FSIV to be classified as SIC component. In this context, the Table 3 shows additional examples of reported uses of FIVs and gate valves in different facilities.

Table 3. Summary of experimental research about FIV uses in accelerator facilities.

Research	Objectives	Setup	Results
The SPIRAL2 facility at GANIL [10].	This facility uses FIVs classified as a Safety Component to protect against air-inrush and radioactive products.	• FIVs DN100 from VAT. • Safety Interlock to shutdown the beam integrated through two redundant subsystems logic gates and relays (and a PLC for general control) • x4 FIVs installed in several beam lines.	• Time for closing of valves between 10-25 ms (triggered by plasma discharge gauges) • The system coupled with a fast beam shutdown subsystem.

AIRIX Accelerator linear electron.	The AIRIX accelerator is a linear electron accelerator that uses intense electron beams to produce X-rays for military purposes.	• FIVs DN160 from VAT. • FIVs were used to protect the accelerator from shrapnel and gas coming from the tantalum target when is destroyed.	Valves were used over the period 2000 - 2011 and were found to be very reliable devices even in harsh conditions.
Safety Instrumented Systems (valves) for AWAKE at CERN [11]	Gate Valves (no FIVs) are used to isolate rubidium inside the plasma vacuum cell in AWAKE by closing the valves in front of view ports in case a leak in the chamber is detected.		Standards IEC 61508, IEC 61511 and ISA 84 to achieve a SIL 3 for this safety instrumented function

In addition to the summary tables, there are other related studies which were not included in the previous literature review and are described hereafter:

The study of ref. [12] describes a series of experiments carried out at Raja Ramanna Centre for Advanced Technology (India) to simulate the process of accidental vacuum failure in a 10 MeV electron LINAC. The goal was to investigate various methods for fast detection of vacuum failure and subsequent inhibition of radio frequency pulses to prevent damage to the LINAC. The response time of the interlock (FIV) from the detection of the pressure gauge was 160 ms, but the ion current of the gauge was found very sensitive to vacuum changes and responded quickly. An interlock (FIV) circuit was designed that senses the ion current signal of the pressure gauges and stops the master trigger system of the LINAC in less than 3 ms after rupture of the foil.

In XFEL facility [13], DN100 fast-closing valves of the flap type are used to secure the operation of the beam transport vacuum system that guides the X-ray beam to scientific instruments in case of a sudden air inrush. These valves are installed 27 m upstream the separation chamber and are triggered by a redundant system of two cold cathode sensors, located 30 m away for fast reaction. At the windowless interfaces to the accelerator vacuum system, smaller DN40 valves of the linear actuator type are used, triggered by a pair of redundant sensors on each side. These valves protect both the accelerator and photon vacuum sides. All valve controllers are connected to the machine protection system which revokes beam permission within 25 ms to prevent the valves from being hit by the beam. The closing time of the valves is around 10 ms and trigger level is set at $5 \cdot 10^{-6}$ mbar.
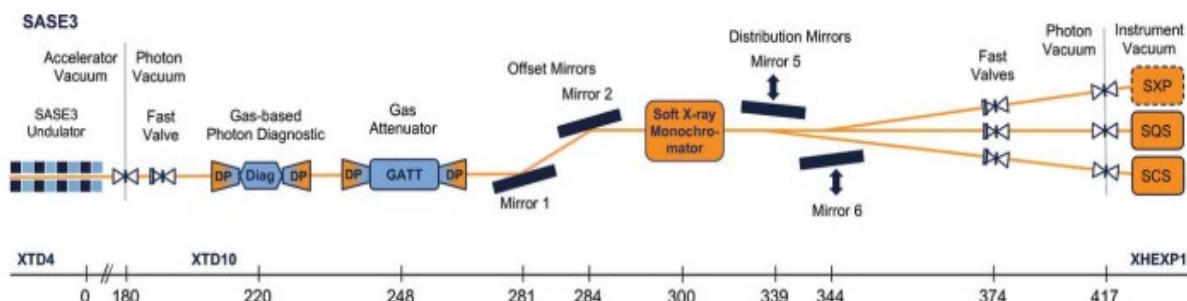
Figure 1. Schematic overview of the photon vacuum system. UHV sections are indicated in orange colour [13]

Finally, in 2011 the vacuum group of the Brookhaven National Laboratory conducted a study (ref. [14]) evaluating the time response of different pressure gauges in a controlled air-in-rush condition, with the aim to prevent damages to the vacuum systems. First, they characterized the time of travel of the gas front in vacuum at a known distance after inducing the rupture of an aluminium foil. The response times of the pressure gauge from the rupture to reach 10^{-7} Torr (~10 mbar) were around 12-13 ms (IKR 070), and 3-4 ms (MKS 442 CCG). Finally, a theoretical result of the time of travel of the gas front over the distance was presented using the most probable velocity equation, as a time estimation of 2 ms.

3. Technical Design of the MuVacAS Experimental Setup

This chapter describes the functional specifications and technical design of the MuVacAS setup. The first aspect to be considered is that the setup shall recreate as much as possible the geometry of the High Energy Beam Transport line (HEBT) and the Target Vacuum Chamber (TVC) of the IFMIF-DONES accelerator. Therefore, this chapter presents a comparison between the geometry of the IFMIF-DONES HEBT+TVC and MuVacAS. In addition, the main experimental objective of the MuVacAS is to recreate the three RAS identified in the introduction. For this purpose, three experimental modules are proposed. For the case of RAS#5, a sudden air inrush system was conceived to recreate an eventual rupture of the TVC backplate. For the cases RAS#12 and RAS#13, the proposal involves the integration of a water injection module and a gas injection module respectively, which can be connected at specific points along the line to recreate the scenarios. The use of fast acquisition systems (including fast pressure acquisition) is essential to record these events and to estimate front propagation speeds. Furthermore, the MuVacAS setup shall integrate FSIVs to test them as mitigation mechanism, while other eventual mitigation measures such as baffles or acoustic reductors may be proposed for further investigations. Finally, MuVacAS is a multipurpose setup, and its complementary objective involves testing characteristics of the HEBT vacuum design (such as Differential Pressure System), as well as the performance of vacuum component prototypes designed ad hoc for IFMIF-DONES.
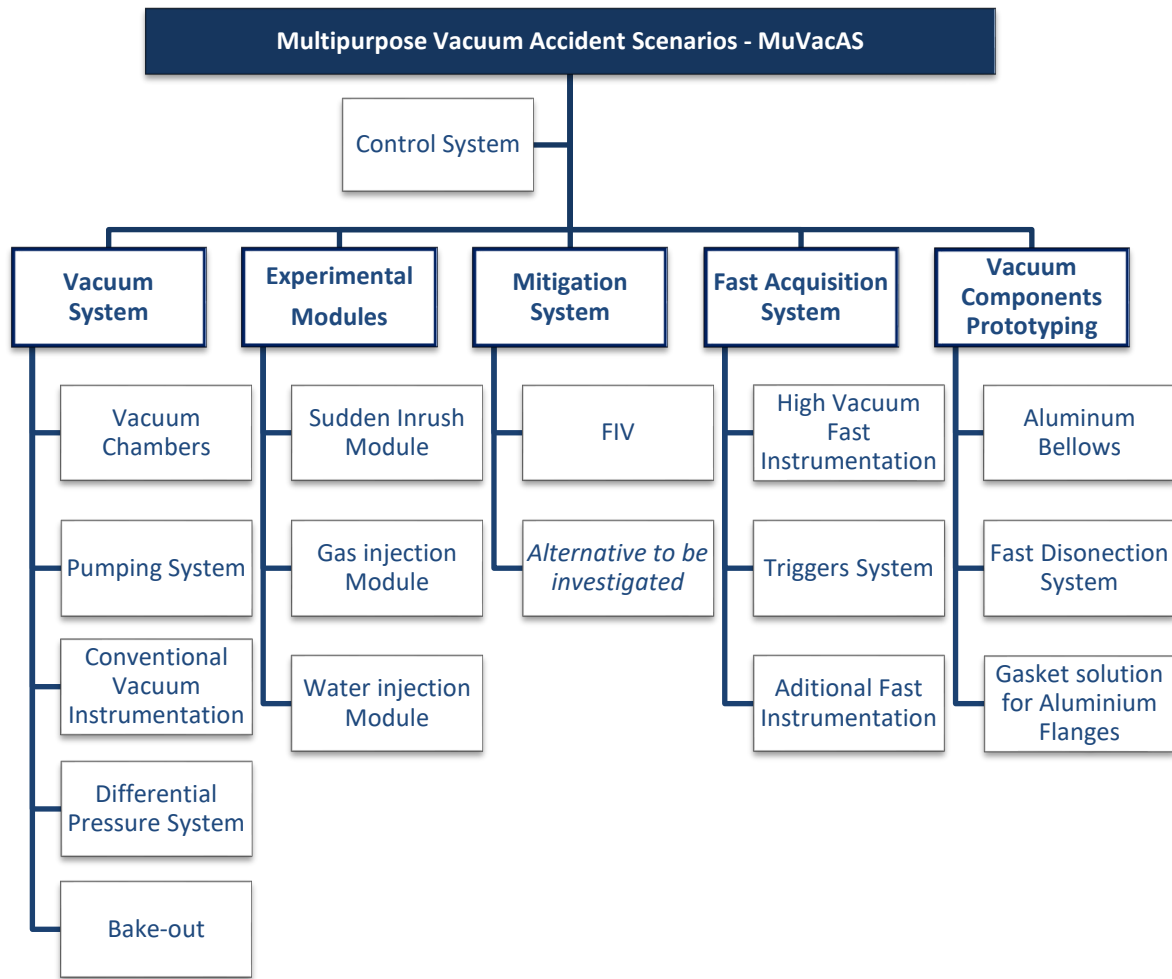
Figure 2. Sketch of the Breakdown Structure of MuVacAS Setup.

Figure 2 shows a schematic breakdown structure of the MuVacAS systems, based on the conceptual aspects described.

The geometry of the MuVacAS shall be as similar as possible to the IFMIF-DONES HEBT. However, this is not practically possible due to space limitations since the total length of the HEBT is 49 m. For this reason, a scale-down of the MuVacAS setup is necessary. To minimize the differences in the scaling-down process, the MuVacAS setup has been divided in two separated zones, Zone A and Zone B. This is shown in Figure 3, together with the geometry of the IFMIF-DONES HEBT. The Zone A is the upstream part and has a longitudinal scale of 1:2.5 with respect to the HEBT (i.e, a length of 14 m in MuVacAS represents a length of 35 m in the HEBT). The Zone B represents the equipment downstream the FSIV 2, down to the back-plate of the TVC. The scale of this zone is close to 1:1 since it is the most critical part for the RAS studies envisaged. This nomenclature of zones is used across the document. Each zone is subdivided in different sectors (A1, …, A8, B1, …, B5), which can be isolated by gate valves.
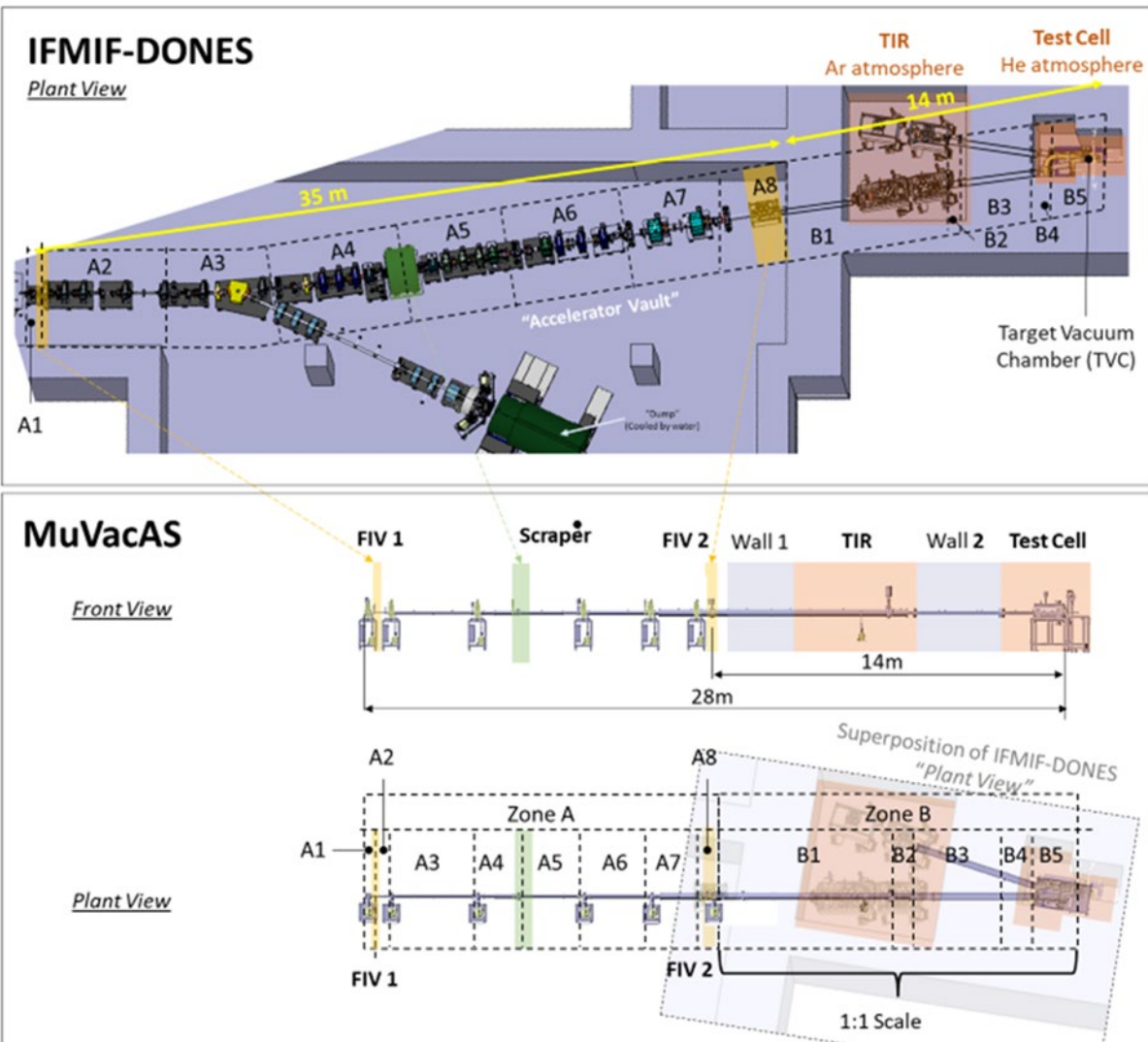
Figure 3. Diagram presenting a footprint to compare IFMIF-DONES and MuVacAS.

Figure 4 shows a rendering of the detailed design of the MuVacAS setup. The following sections will detail the conceptual specifications and technical solutions for each of the subsystems of the setup according to the Breakdown Structure of Figure 2.

Figure 4. Render of MuVacAS experimental setup

3.1 Vacuum System

The Vacuum System (VS) of the MuVacAS setup is composed of three main vacuum chambers:

1) The Control Volume Vacuum Chamber (CVVC): This chamber is located in Zone A1 and facilitates precise measurement of the amount of incoming air upstream of the vacuum line. High vacuum pressure close to 10^{-8} mbar is required in this area to recreate the connection to the cryomodules in the HEBT.

2) The vacuum line: This line represents the HEBT geometry in terms of its duct diameters according to the most updated HEBT-CAD [15].

3) The Target Vacuum Chamber (TVC): This chamber is located in Zone B5. The main geometrical characteristics are taken from the TVC CAD [16]. Its pressure should be kept between 10^{-4} and 10^{-5} bar [17] through the Ar injection system as required in IFMIF-DONES to avoid Li boiling.

The VS is equipped with different Pumping Units (PU) along the line, with their isolation valves to protect them during the experimental campaigns (gas inrushes). In addition, the pumping system should maintain a pressure gradient along the line from the CVVC to TVC. For doing so, the estimated range of argon gas injection in the TVC to be controlled is within $7 \cdot 10^{-4}$ mbar·l/s (0.04 sccm for target pressure of 10^{-5} mbar) and $4.5 \cdot 10^{-3}$ mbar·l/s (0.3 scmm for target pressure of 10^{-4} mbar) [17]. To allow some margin, the specified range for the TVC Ar injection system has been established within 0.01 and 1 sccm.

The VS has conventional vacuum instrumentation such as pressure gauges (Cold Cathode and Pirani), and Residual Gas Analyser (RGA). The RGA can be used to identify the composition of residual gases, as well as the partial pressure of each gas. Also, the VS is equipped with a bake-out system, which facilitates and accelerates the outgassing to reach the necessary pressures.

The following subsections described the technical design of the main features of the VS.

3.1.1 Geometry of the Vacuum System

Figure 5 shows the VS including the vacuum chambers (CVVC, vacuum line and TVC), six pumping units (PU) and seven Gate Valves GV. Furthermore, the VS comprises also the differential pressure system (through controlled Ar injection in the TVC), pressure instrumentation, and a bake-out system distributed along the 28 m long MuVacAS line. The complete MuVacAS diagram is presented Appendix 2: Diagram of MuVacAS.
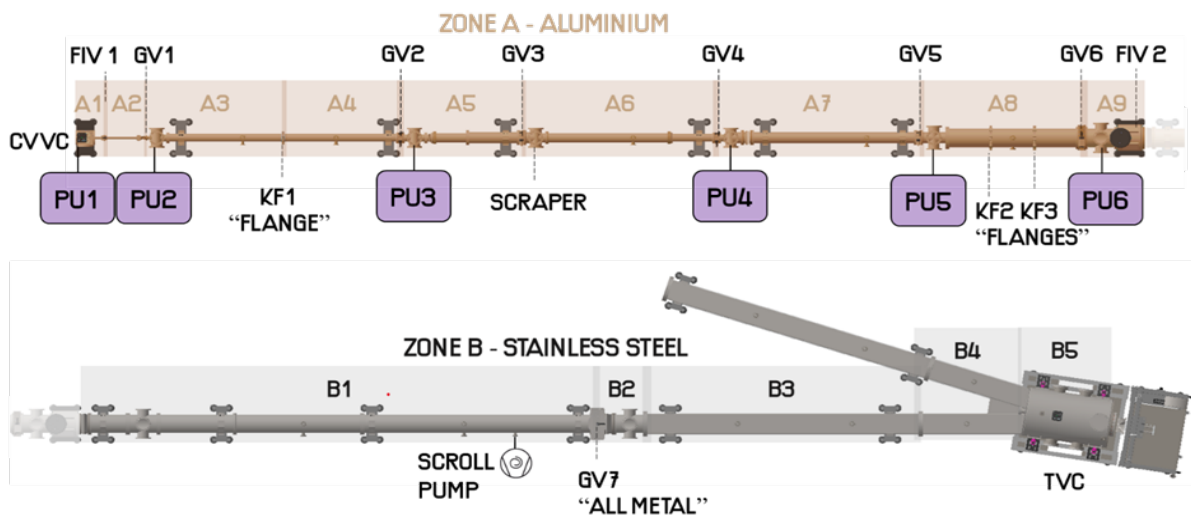
Figure 5. Distribution of the Vacuum System.

Table 4 shows a comparison of dimensions between the zones of the HEBT and MuVacAS as defined in the Figure 3. In the zone A and zone B different materials were selected for the vacuum chambers, aluminium for Zone A, and Stainless-Steel AISI 304L for Zone B, consistently with the current HEBT design (although in the HEBT the steel grade will be AISI 316L [18]). Most of the fixed flanges used are ISO CF flanges with diameters ranging from DN40 to DN250. In addition, some KF-like flanges will be placed in specific locations for evaluating its eventual implementation in the final HEBT design.

Table 4. Vacuum line comparison between IFMIF-DONES and MuVacAS

Zone	Start	End	IFMIF-DONES (m)	MuVacAS (m)	Diameter
Zone A1	CVVC	FIV1	0.41	0.81	DN 40
Zone A2	FIV1	GV1	6.98	0.45	DN 40
Zone A3	GV1	GV2	4.7	3.45	DN 100
Zone A4	GV2	GV3	5.36	1.59	DN 100, DN 130, DN160
Zone A5	GV3	GV4	5.4	2.54	DN 130, DN 100
Zone A6	GV4	GV5	5.69	2.64	DN 160
Zone A7	GV5	GV6	3.57	2.15	DN 160, DN 250
Zone A8	GV6	FIV2	2.89	0.73	DN 250
Zone B1	FIV2	GV7	7.28	**6.9**	DN 250
Zone B2	GV7	Rect. Pipe	0.65	**0.55**	DN 250
Zone B3	Rect. Pipe	Rect. Pipe - TVC	4	**3.6**	270x120 mm *
Zone B4	Rect. Pipe - TVC	TVC	1	**1.3**	270x120 mm *
Zone B5	TVC	TVC - Back plate	1.07	**1.13**	Ø 660 x 1135

| | Total | 49 | 27.84 | *Internal Area* |

3.1.2   Control Volume Vacuum Chamber

The CVVC consists of a cube of stainless steel of 5 l volume, with three of its faces closed by three DN160 CF Blank Flanges, and the remaining connected to the vacuum line. A FIV DN40 with a CF flange is placed in the connection with the main line as shown in Figure 6. On the top of the cube a pressure gauge and a RGA are connected.
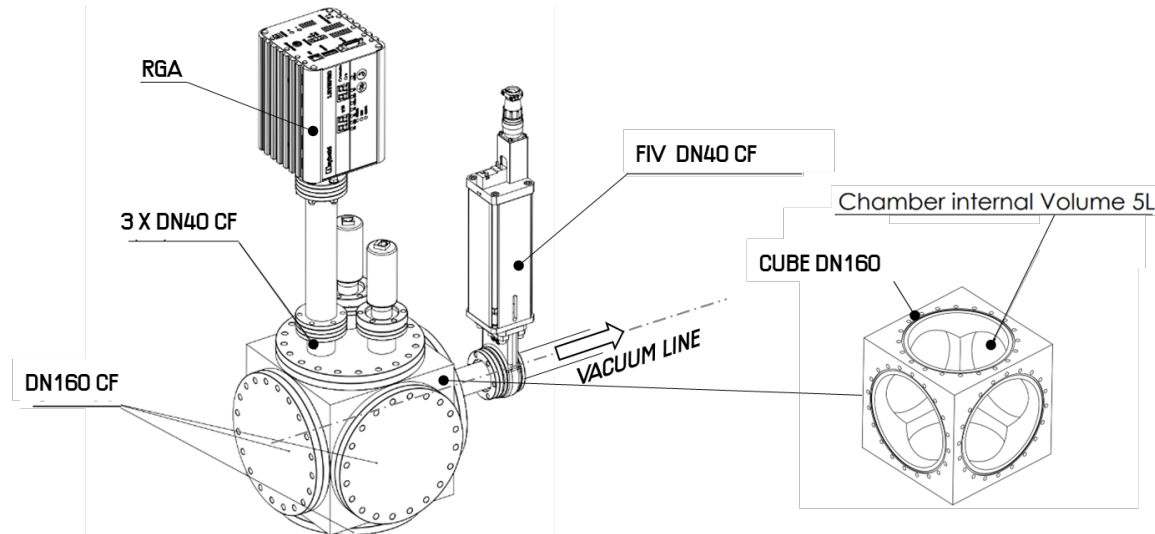
Figure 6. Main components connected to the CVVC.

3.1.3   Target Vacuum Chamber

Figure 7 shows the current design of the MuVacAS TVC. The main dimensions of the version of the IFMIF-DONES TVC have been considered (such as: diameter = 600 mm, length = 1135 mm) [16]. At the same time, several modifications have been made to adapt the chamber to experimental tests recreating back-plate rupture (open Flange DN275 CF) and the eventual integration of instrumentation with the following flanges: 3 x Flanges DN40 CF, 4 x Flange DN160 CF and 2 x Flange DN200 CF. The TVC will be manufactured on Stainless Steel 304L with a wall thickness of 1 cm.
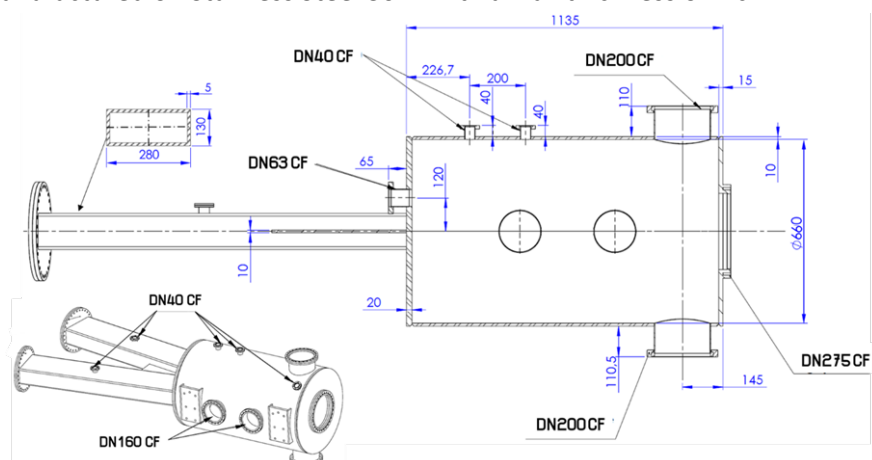
Figure 7. Drawing and main characteristics of the TVC (units: mm).

During the design of the TVC it was observed that the mechanical stresses due to vacuum ($\sigma_{VM,max} = 279$ MPa) exceed the yield stress of the material ($\sigma_{YS} = 210$ MPa). For this reason, a rib connecting the two rectangular tubes was added to reduce the stresses as shown in Figure 8. Maximum stress with the ribs is $\sigma_{VM,max} = 127$ MPa, meeting the mechanical design compliance.
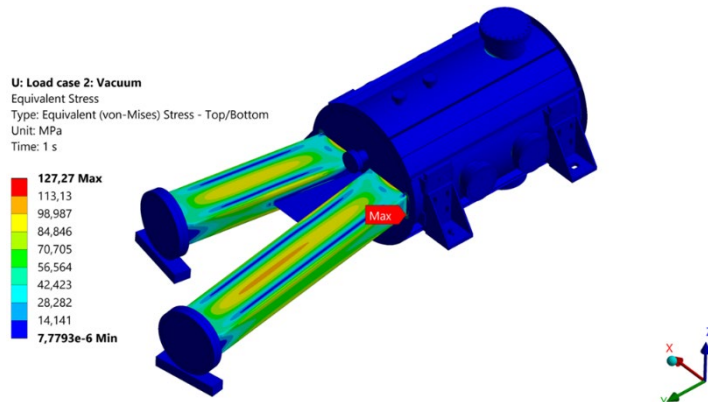
Figure 8. Equivalent von-Mises Stress of the TVC under vacuum.

3.1.4 Pumping Units

There are six Pumping Units (PU) distributed along the vacuum line as shown in the Figure 5. Each of these units is equipped with the elements presented in the Figure 9 and explained in detail below.
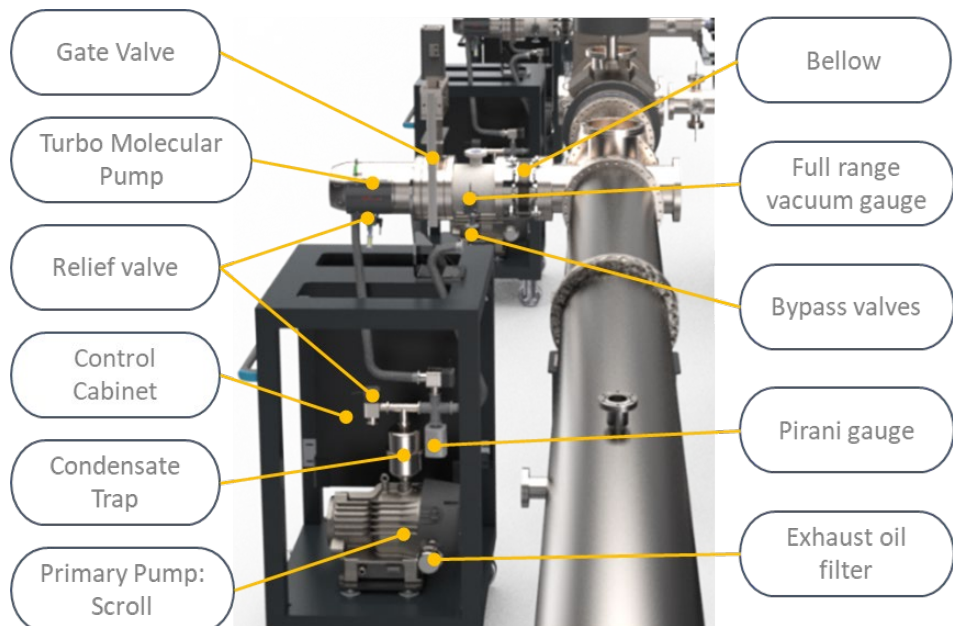
Figure 9. Main parts of the pumping unit.

<u>Primary pump</u>: Edwards nXDS15i Scroll pump with a peak pumping speed of 4.2 l/s. The pump is controlled through a digital and analogy input/output interface called "Parallel Control", and this is connected to the control cabinet.

<u>Turbo-Molecular Pump (TMP)</u>: LEYBOLD TURBOVAC 450 iX with the pumping characteristics showed in the Table 5. The pump has a relief valve driven by the pump controller and can have a DN160 CF -

230V band heater if necessary to reach the specified vacuum levels. This pump model can be installed in any position and orientation. In addition, the PROFIBUS DP interface controls and monitors various parameters of the turbomolecular pump.

Table 5. Pumping characteristics of TURBOVAC 450 iX for different gases.

Gases	Pumping speed (l/s)	Gas throughput (mbar·l/s)
N_2	430	4.5
Ar	400	2.0
He	440	8.0
H_2	420	8.0

Vacuum valves: This group consists of bypass valves, relieve valves (between the primary and turbo pump) and a gate valve to isolate the pumping unit from the line. The opening and closing of these valves will be controlled electronically and their status will be monitored through the position end-stops incorporated in each valve.

There are other auxiliary components as condensable vapour trap added to each pumping unit at the inlet of the Primary Pump to minimise the amount of water vapour reaching the pump. This is done to protect the pump after water injection tests, minimising the risk of pumping large quantities of water that could cause condensation inside them. Furthermore, each PU are connected to the vacuum line by a bellow of Stainless-Steel, which allows the expansion and misalignment between these both systems.

3.1.5 Conventional Vacuum Instrumentation

Each pumping unit will have a Full Range (FR) pressure gauge ("Pirani" + "cold cathode") to monitor the pressure at the TMP pump inlet and one Pirani gauge to monitor the pressure at the TMP pump outlet and in the previous vacuum line (Table 6). These sensors will have a PROFIBUS DP connection to connect them to the main controller. Additionally, one RGA will have the option to be interchangeable of position between the CVVC and the TVC. These locations are presented in Appendix 2: Diagram of MuVacAS.

Table 6. Conventional vacuum instrumentation.

Type	Etiquette	Reference	Quantity
Full Range pressure gauge	FR	TBD	6
Pirani pressure gauge	PI	TTR91RN	6
Residual Gas Analyser	RGA	LEYSPEC VIEW 100S	1

3.1.6 Differential Pressure System

The Differential Pressure System consists in an Argon injection system composed of a Mass Flow Controller (MFC) witch a range of 1×10^{-4} - 1 sccm and a valve (BK series) from Swagelok. Both parts have VCR connections from Swagelok to be fully compatible with the UHV line. VCR connection is a face seal type fitting which uses copper gasket for sealing, like a CF connection used in UHV systems.

The injection will be carried out by a closed loop control, considering the pressures of the TVC and CV chambers to keep them within their limits (TVC $10^{-5} - 10^{-4}$ mbar by modifying the flow setpoint of the MFC.

To estimate the flow range needed for the MFC, numerical analyses have been performed in MolFlow+ with the current geometry of the high-vacuum line. The first estimates consider different argon injection flow rates. The profile is similar to the one estimated for the IFMIF-DONES HEBT line. The system will take measurements from several pressure gauges along the line to dynamically control the pressure in the TVC between 10^{-5} and 10^{-4} mbar, while the pressure in the Zone A1 is around $5 \cdot 10^{-8}$ mbar. The system will inject Ar within a flow rate of $7 \cdot 10^{-4}$ mbar·l/s (0.04 sccm for a pressure in the TVC of 10^{-5} mbar) and 4.5×10^{-3} mbar·l/s (0.3 sccm for a pressure in the TVC of 10^{-4} mbar).
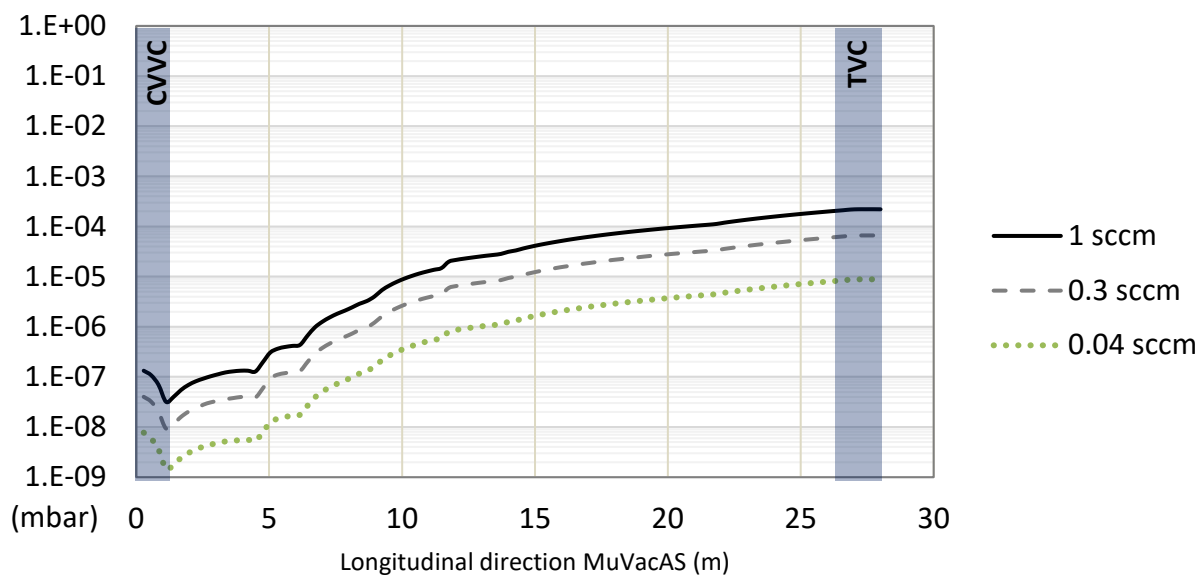
Figure 10. Estimated pressure along the high vacuum system for different Ar injection flow.

3.2 Experimental Modules

The MuVacAS setup is equipped with three main experimental modules at different locations along the line to recreate vacuum loss scenarios. Their instrumentation and the triggering of the actuators are synchronized with the central acquisition system.

3.2.1 Sudden Air Inrush Module

This setup will be used to recreate sudden gas inrushes in case of the TVC backplate rupture, as well as eventual duct seizures upstream the FSIV. To represent the backplate in the TVC and its rupture, a DN275 mm flange with exchangeable Al foil windows is added (as shown in Figure 7). In addition, this foil window configuration could be also integrated to a duct upstream the FSIV.

The sudden air inrush module is composed of a pendulum which is dropped onto the aluminium foil (Figure 11) when the chamber is under vacuum. This generates a rupture on the foil, which causes a sudden air inrush. The integration of the aluminium foil in the DN275 CF flange is achieved through a copper seal - AL1015 foil - copper Seal - DN275 CF flange – Bolts.

The system is also equipped with a trigger and dedicated instrumentation to detect the instant of impingement and define "time 0" of the inrush. This system will allow the study of reaction times of the mitigation systems is RAS #5, as well as the measurement of wave fronts propagation.

The fall of the pendulum is released by a pneumatic actuator and can therefore be operated remotely. Also, it is equipped with an encoder coupled to its shaft mechanism, which allows angle measurement with a resolution of 0.036° and the synchronisation of the data acquisition systems. Four punch geometries have been designed for the pendulum to recreate different types of ruptures, as shown in Figure 11.
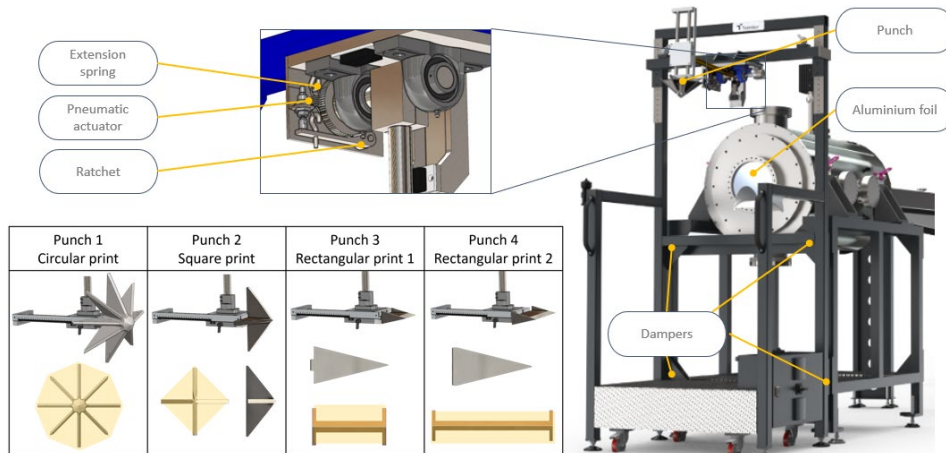
Figure 11. Mechanism to actuate remotely the punch pendulum.

Some design parameters of the aluminium foil that were not possible to predict by numerical solutions were obtained through experimental tests. This is the case of the foil thickness that shall mechanically resist the vacuum forces without failing, while allowing its suitable rupture by the pendulum punch with enough repeatability. The experimental studies presented in section 4.1.2 lead to the selection of a foil thickness of 0.5mm, while thicknesses of 0.3 and 0.7 mm were also tested.

3.2.2   Gas Injection Module

The second experimental module is dedicated to recreating small leaks of different gases such as air, N_2, He and Ar (consistent with the RAS #13). The module uses an intermediate gas chamber connected to the vacuum line through a regulated leak valve (Mass Flow Controller) and a fast solenoid electro valve that is capable of opening and closing in the millisecond range (10 ms). The system is able to measure the mass rate and total amount of injected gas, set in the range from 0.01 g/s to 40 g/s, and it is connected to the fast acquisition system to synchronize the trigger with the pressure measurements along the line. Table 7 shows an equivalence of volumetric flow for different gasses corresponding these mass flow ranges.

Table 7: Equivalence of gas flow mass rates and volumetric range, and maximum injection times based on 10 l, 200 bar bottle.

	Air	Ar	N_2	He
Density g/l 15 ºC	1,225	1,69	1,185	0,167
GCF	1	1,39	1	1,45
0.01 g/s				
l/s	0,008163265	0,00591716	0,008438819	0,05988024
sccm	489,7959184	355,0295858	506,3291139	3592,814371
N_2 sccm	489,7959184	255,4169682	506,3291139	2477,803015
Maximun injection time (min)	4000	5520	3871	545
40 g/s				
l/s	32,65306122	23,66863905	33,75527426	239,5209581
sccm	1959183,673	1420118,343	2025316,456	14371257,49
N_2 sccm	1959183,673	1021667,873	2025316,456	9911212,059
N_2 slm	1959,183673	1021,667873	2025,316456	9911,212059
Maximun injection time (s)	60	82	58	40

The gas injection system has been designed to have everything mounted in a small trolley that can be moved and connected to any of the crosses and chambers of the Muvacas UHV line (as shown in Figure 12). The system has one 10 l and 200 bar gas bottle (Alphagaz 1 from Air Liquide) installed in one side of the trolley. It is connected directly to a pressure reducer (RSH8 from Swagelok) and gas distribution system. The pressure reducer has been designed to be able to have the maximum flow of 2000 slm N2 for the different gases from 200 bar down to 4 bar, which is the output pressure of the reducer. Both the pressure reducer and the manifold are of 1" size to reduce the pressure drop.

The gas manifold is connected directly to different valves by means of 12 mm tubes. These valves, BK series from Swagelok with VCR ports, have been selected due to the low response time and full compatibility with vacuum systems. Response time of less than 20 ms were measured when using the 808 model Pneumax electro valve and 6 bar of air pressure (10 ms was also obtained with an input air pressure of 10 bar). The electro valve is mounted just in the vicinity of the gas valve to reduce the length of the piping which must be less than 100 mm. Each Swagelok valve will have a position indicator switch which will indicate that the valve is fully open.

Each MFC has its own BK Swagelok valve with the same port connection of the MFC. But, for the 2000 SLPM, with 1-inch VCR port connection, no VCR valve was available, so a gas collector has been designed to include up to five ½ inch VCR valves. The ½" VCR valve has a Cv maximum of 0.96, so with an inlet pressure of 4 bar and an output pressure of vacuum, a flow of around 600 slm for Ar (which is the worst case, other gases have more flow) is possible for each valve. So, at first 4 valves will be installed for a total flow of 2400 slm.

3 fast mass flow controllers (MFC) from Alicat MC series, response times low as 30 ms, are going to be used. The range for each MFC is the following (from the minimum flow to the maximum):

• 5 SLPM MFC: 255 sccm – 5 SLPM N2.
• 100 SLPM MFC: 5 – 100 SLPM N2.

• 2000 SLPM MFC: 100 – 2000 SLPM N2.

Table 8. Flow ranges and error estimators of the MFC in the gas injection module.

Flow Ranges	5 SLPM	100 SLPM	2000 SLPM
FS	0.15	1	5
Error spec, %FS	2	2	2
.			
Flow rate to measure	[0.255 - 5]	[5 - 100]	[100 - 2000]
Error, SLPM	[0.005 - 0.03]	[0.24 - 1]	[4.8 - 20]
AND/OR	AND	AND	OR
Error, %RD	**0.60 - 1.96 %**	**1.00 - 4.80 %**	**1.00 - 4.80 %**
.			
Totalizer signal accuracy, SLPM	[0.006275 - 0.055]	[0.265 - 1.5]	[5.3 - 30]
Totalizer signal accuracy, %RD	**1.1 - 2.46 %**	**1.5 - 5.3 %**	**1.5 - 5.3 %**
.			
Analog signal accuracy, SLPM	[0.01 - 0.035]	[0.34 - 1.1]	[6.8 - 22]
Analog signal accuracy, %RD	**0.70 - 3.92 %**	**1.10 - 6.80 %**	**1.10 - 6.80 %**

These MFC not only control and measure the flow but they also integrate the total volume of gas. These MFC have a 1 kHz analogue sample rate so flow measurements every 1 ms can be obtained. Each MFC can be configured with the gas type to inject, so the flow data given by the MFC will be already converted to the gas type, no additional conversion will be required. Table 8 shows ranges and errors of the three MFCs integrated in the module.

1 Pressure reducer
2 Gas manifold
3 Gas bottle

1 Compressed air electrovalves
2 MFC
3 4 way reducer cross
4 Viewport
5 Swagelok BK valves
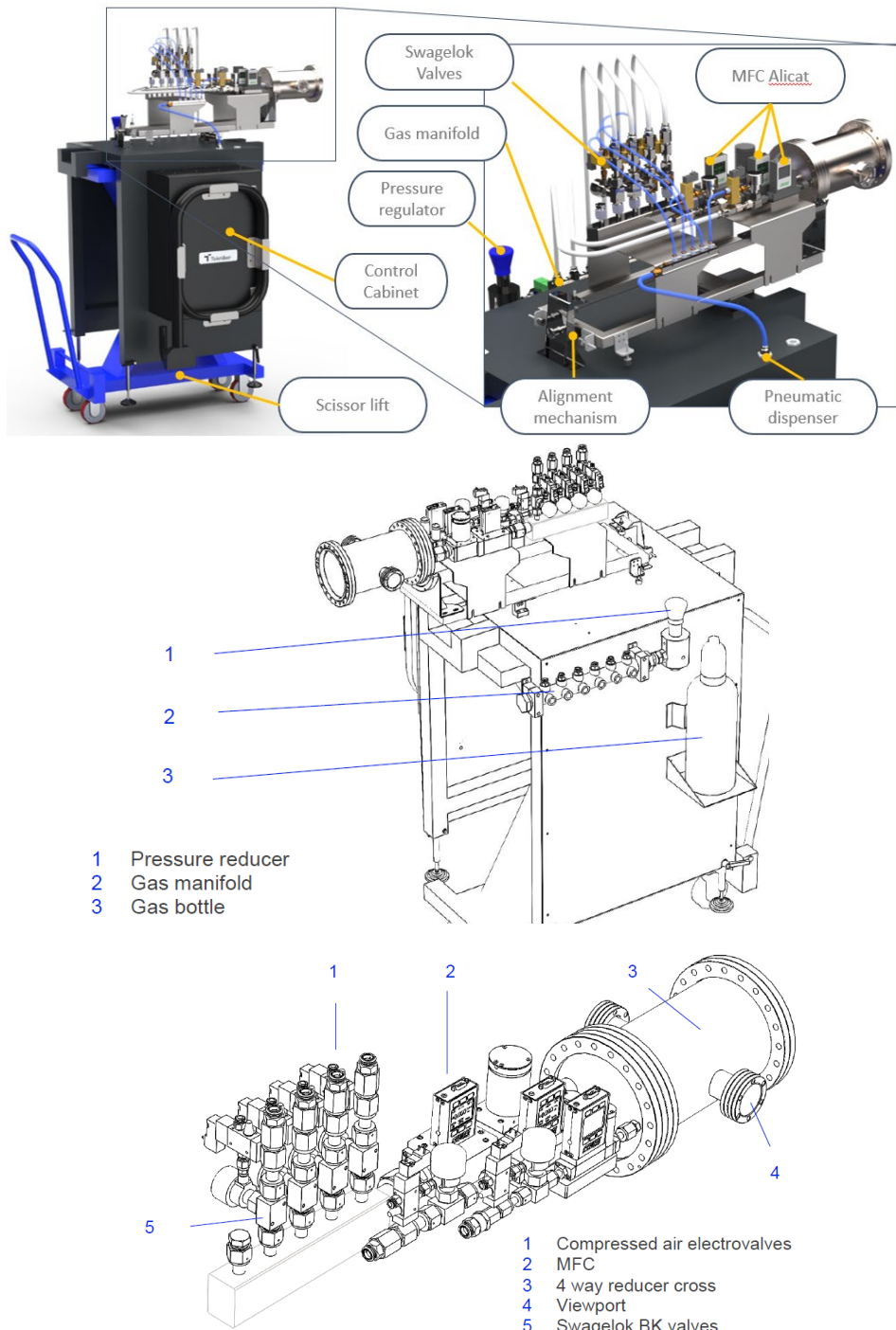
Figure 12. Gas Injection Module and main parts.

3.2.3 Water Injection Module

The objective of this system is to be able to inject demineralised and purified water at a point in the line, being able to recreate from a small water leak (from 0.1 ml/s to 75 ml/s) to an abrupt break (2 l/s) in a pipe, corresponding to the leaks from HEBT scrapers in the RAS#12.

Similarly to the gas injection module, the water injection module (Figure 13) has been designed to be mounted on top of trolley which can be connected to any of the crosses along the vacuum line.

In one side of the trolley the water tank and distribution piping system are located. All the components have been selected to be fully compatible with ultra clean water (stainless steel parts and plastic). The piping size is 1 ½" to minimize pressure drops. The water supply works as follows. A water micropump (1 l/min @ 20 bar) fills the water accumulator from 9 bar to 16 bar to have 10 litres of pressurized water available for the injection. The filling process will be controlled with a pressure sensor from IFM (0-25 bar and 3 ms response time).

After the accumulator, a membrane pressure reducer from BERLUTO (output pressure 1.5-10 bar) will reduce the pressure to the 8 bar needed in the injection. Another membrane pressure reducer (output pressure 0.5-4 bar) reduces the pressure from the 8 bar to the 2 bar needed by the MFC. Both pressure reducers have their own visual manometer, and they are fully adjustable to other output pressures. The output pressure of the first pressure reducer is monitored by and IFM pressure sensor (0-10 bar and 3 ms response time), this would allow to check the pressure drop during the injection and adjust it to different injection flows.
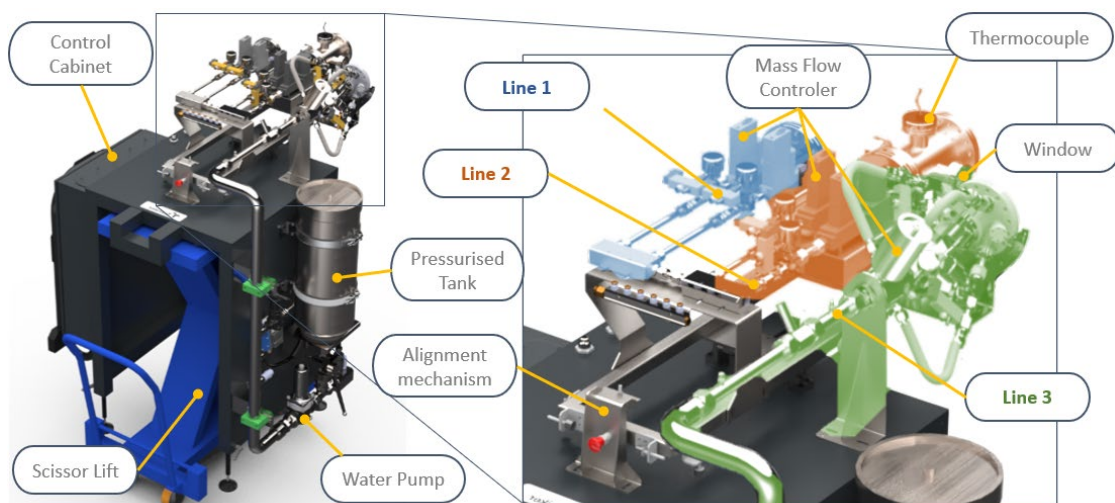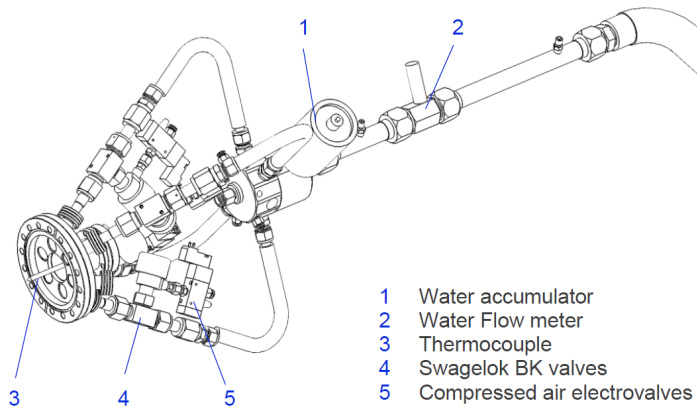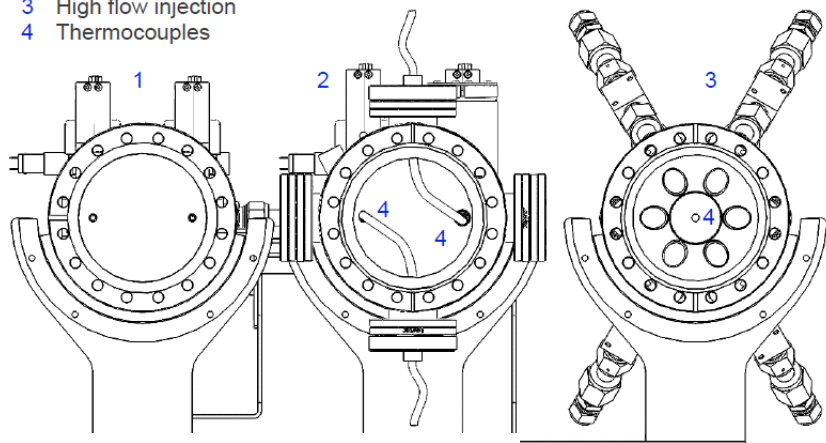
Figure 13. Water injection module and main parts.

Due to the range of the flow rates required, it has been divided into three lines, each with its own CF100 connection flange, as shown in Figure 14.

1 Low flow injection
2 Medium flow injection
3 High flow injection
4 Thermocouples

1 Water accumulator
2 Water Flow meter
3 Thermocouple
4 Swagelok BK valves
5 Compressed air electrovalves

1 Swagelok BK valves
2 MFC
3 Thermocouple
4 Compressed air electrovalve
5 Viewport
6 6 ways reducer cross
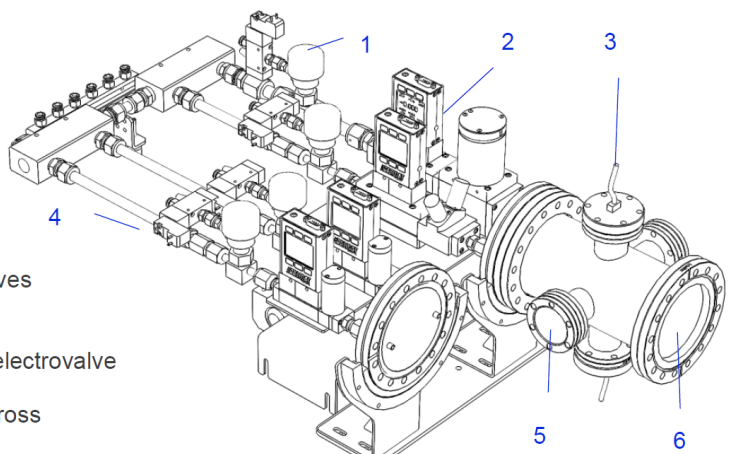
Figure 14: View of the 3 different injection subsystems of the Water Injection Module

For the injection subsystem 3, the one for 120 litre per minute, no closed loop is envisaged. The amount of flow will be adjusted by means of the pressure output of the first pressure reducer and the number of valves opened. 4 ½" valves from Swagelok that have been installed. With an input pressure of 8 bar and output pressure of vacuum, each valve can supply around 39 l/min. So, 3 of them will be necessary to have around 120 l/min. Each valve can be operated independently of the others so, the minimum flow with 1 valve opened and an input pressure of 2 bar, will be 19.5 litre per minute. The maximum

flow with the 4 valves opened and an input pressure of 8 bar, the maximum allowed inlet pressure at the Swagelok valves, will be 156 litre per minute. (theoretical limit values). Upstream and and as close as possible to the valves, a water flow meter from TrigasDM has been installed. This turbine type water flow meter can measure flows from 19 to 220 l/min with a response time of less than 3 ms and a linearity error of less than 0.1% of reading value. This is possible by using their own electronics system and the flow conditioner tubes at the inlet and outlet of the flowmeter. The total volume injected in this subsystem can be calculated with two different methods. The first method is integrating the flow measured by the water flowmeter along the time. the second method is comparing the pressure reading by the IFM sensor.

The other two water injection subsystems (1 and 2) are very similar each the other, having each of them x2 LFC (liquid flow controller) for water flow control in a CF100 flange. In total, 4 fast mass flow controllers (LFC) from Alicat LC series, response times low as 30 ms, are going to be used. The range for each MFC is, from the minimum flow to the maximum:

• 25 CCM LFC: 6 – 25 ccm (0.1 - 0.4166 ml/s).
• 150 CCM LFC: 25 – 150 ccm (0.4166 - 2.5 ml/s).
• 1 LPM LFC: 150 ccm – 1 LPM (2.5 - 16.666 ml/s).
• 5 LPM LFC: 1 – 4.5 LPM (16.666 - 75 ml/s).

These LFC not only control and measure the flow but they also integrate the total volume of injected liquid. These LFC have a 1 kHz analogue sample rate so flow measurements every 1 ms can be obtained.

The selection criteria for the total amount of MFC and their control range was based on the error of the measurement to be less than 15%, both in the analogue signal and in the totalizer (Table 9).

Table 9. Flow ranges and error estimators of MFC in the water injection module.

Flow Ranges	25 CCM	150 CCM	1 LPM	5 LPM
FS [LPM]	0.025	0.15	1	5
Error spec, %FS	2	2	2	2
Flow rate to measure [LPM]	[0.006 - 0.025]	[0.025 - 0.15]	[0.15 - 1]	[1 - 4.5]
Error, SLPM	[0.0005 - 0.0005]	[0.003 - 0.003]	[0.02 - 0.02]	[0.1 - 0.1]
Error, %RD	**2.00 - 8.3 %**	**2.00 – 12 %**	**2.00 - 13.3 %**	**2.22 – 10 %**
Totalizer signal accuracy, SLPM	0.00053	0.003125	0.02075	0.105
Totalizer signal accuracy, %RD	**2.5 - 8.83 %**	**2.5 - 12.5 %**	**2.5 - 13.83 %**	**2.72 - 10.5 %**
Analog signal additional error spec, %FS	0.1	0.1	0.1	0.1
Analog signal accuracy, %RD	**2.10 - 8.75 %**	**2.10 - 12.6 %**	**2.10 - 14 %**	**2.33 - 10.5 %**

3.3 Vacuum loss Mitigation System

3.3.1   Fast Isolation Valves

The Fast Isolation Valves (FIVs) are the main mitigation element of the MuVacAS setup, and it is built to validate this component. Initially, the setup will be equipped with two FIVs provided by VAT (as showed in Figure 5). One DN-40, located downstream to the CVVC, and one DN250, located in the position corresponding to the RIR in the real HEBT. However, the number of FIVs may increase to meet the redundancy requirements of the real facility and due to the fact that the large FIVs are unidirectional. The triggering system of the valves will consist of x2 gauges of the "Glow Discharge" type, for medium pressure (Fine Vacuum), and x2 cold-cathode gauges for low pressure (High Vacuum). The FIVs, gauges and Control system are provided by the company VAT. The cable length used will be equivalent to the ones in the real facility (over 50-100 m). Additionally, the FIVs and their configuration control will be continuously upgraded to meet the detailed reliability requirements and design architecture as the project progresses towards achieving the safety goals.

Table 10. Benchmarking of different VAT FIV flange sizes.

Flange Size	DN 40	DN 100	DN 160	DN 200	DN 250	DN 320
Flange	CF	CF	CF	CF	ISO-F	ISO-F
Conductance [Ls^{-1}]	220	700	1700	2500	5200	8400
Diff Pressure (valve closed)						
In closing direction [bar]	1,2	2	2	2	1,2	1,2
In opening direction [bar]	1,2	1,2	0,5	0,07	0	0
Diff Pressure (at opening)						
In closing direction [*mbar*]	30	180	50	25	25	25
In opening direction [*mbar*]	30	1000	1000	1000	1000	1000
Radiation resistance [Gy]			Body 10^8			
Actuator	10^4	10^4	10^4	10^4	10^5	10^5
Position indicator	10^5	10^5	10^5	10^5	10^6	10^6
gate seal	10^5	10^5	10^5	10^5	10^6	10^6
Bake Out Temperature [ºC]						
Body	200	200	200	200	120	120
Actuator	50	50	50	50	50	**50**
Leak rate Body [mbar ls^{-1}]	10^{-10}	10^{-10}	10^{-10}	10^{-10}	10^{-10}	10^{-10}
Leak rate Seat [mbar ls^{-1}]	10^{-9}	10^{-9}	10^{-9}	10^{-9}	10^{-9}	10^{-9}
Volume actuator [L]	0,36	3	3	3	3	3
Actuation Time						
Closing [ms]	10	15	23	40	70	150
Opening [s]	9	7	7	7	7	7
Weight	2	29	36	42	56	73

Height	466	571	621	679	*700**	904
Width 1 (Dim A)	35	192	242	306	*350**	443
Length (Dim B)	42	200	250	300	*350**	440

Table 10 shows a comparison of different parameters of FIVs models. Above the DN 100 diameter, all the valves work with a flap mechanism, for which the inrush isolation is directional. Other mitigation strategies that may be explored within MuVacAS in the future is the use of baffles for retarding the inrush front wave inside of the line. If this is the case, these baffles will work together with the FIVs, improving their effectiveness by providing extra time for their closing.

3.4 Fast Acquisition Data System

This system will acquire data coming from the pressure gauges, the experimental modules, triggers, accelerometers, and strain gauges. All this information will then be sent to the General Control System.

Several pressure gauges (CC1 to CC24) will be distributed along the line (Appendix 2: Diagram of MuVacAS) connected to the fast acquisition system to measure the gas front propagation and the potential change of its speed depending on the variation of diameter along the vacuum line.

The Fast acquisition System consists of a National Instrument architecture based on a cDAQ-9179 chassis, equipped with a USB3.0 port to connect to the EPICS server, 2 BNC connectors for trigger signal connections and 14 slots to capture all required fast acquisition signals by installing C-series boards. The Ethernet connection consists of a TSN, based on a protocol IEEE802.1 with a synchronization time of less than a 1 microsecond, with a lineal topology. There will be 5 modular systems based on these Compact DAQs from National Instruments:

- 1 module for the gas injection system
- 1 module for water injection system
- 1 module for the pendulum-punch system
- 1 module for accelerometers and strain gauges
- 1 module for quick pressure gauges and FIV valve limit switches

A prototyping campaign has been carried out in order to obtain more information on the capability of the achieving high temporal pressure. Some preliminary results and conclusions obtained are presented in section 4. It seems the preferable solution is achieved by using Pfeiffer IKR050 gauges with a TPG500 controller, from which an analogue signal can be extracted to the analogue-digital converter.

3.5 General Control System

The general control system supervises the whole control of the experimental setup in a centralized manner. A diagram of its proposed architecture and different subsystems in consistency with the elements of the setup is shown in Figure 15. A central PLC SIEMENS S7-1518HF will control all the functionalities of the vacuum system such as pumps, gate valves, monitoring pressures sensors (slow acquisition), differential pressure system, RGA, bake-out, etc., as well as to monitor the state of the FSIVs and eventually force their closing. The PLC will communicate with a centralized computer in which the HMI system will be installed. To optimize the wiring of these elements to the main Siemens

PLC of the general control system, remote Input/Output modules will be distributed throughout the installation. These modules will be connected to the PLC with a single PROFIBUS DP cable. The main Control Cabinet will house the Siemens PLC and the control and monitoring signals of the fixed pumping units, isolated RP pump, conventional guillotine valves, vent valves, and conventional pressure meters. The electrical cabinets associated with mobile pumping unit will also contain a remote I/O module for connecting to the control and monitoring signals of these elements.

The software tools and applications preferably used for the control is EPICS. The General Control System will communicate as well with the Fast Acquisition and Synchronization System, both to control its parameters and to read its recordings after each test. Furthermore, the general control system will be able to communicate with the experimental modules to control the injection of gas/water and to trigger the actuation of the Pendulum-Punch System.
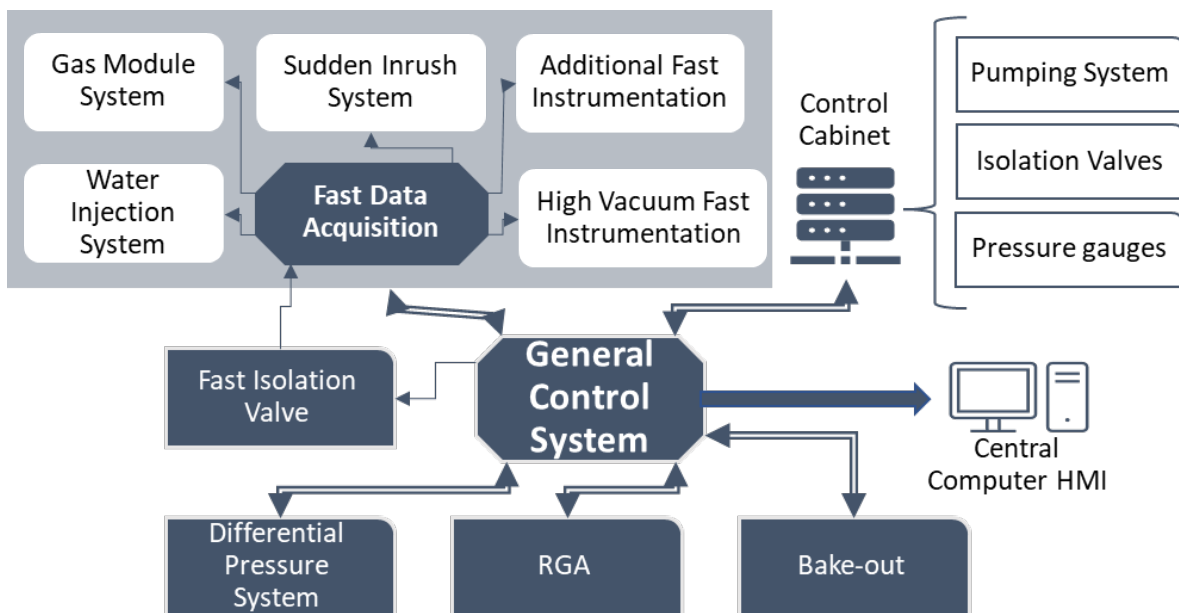

Figure 15. General Control Architecture

4. Prototyping Activities and Preliminary Experimental Results

The first prototype *(called P1)* was built to validate parameters design and verify designs in which there were some uncertainties. P1 consists of a vacuum pipeline with different modules for the installation of pressure sensors at different positions and it has gone through different setups or constructive phases. This section describes four tests carried out by the P1 related with: (i) the validation of the fast response pressure sensors, (ii) the vacuum breakdown tests with the punch pendulum to determine the foil thickness of the window, (iii) the trigger mechanism to detect the initial time where the foil rupture occurs, and (iv) the propagation speed of the front wave in vacuum.
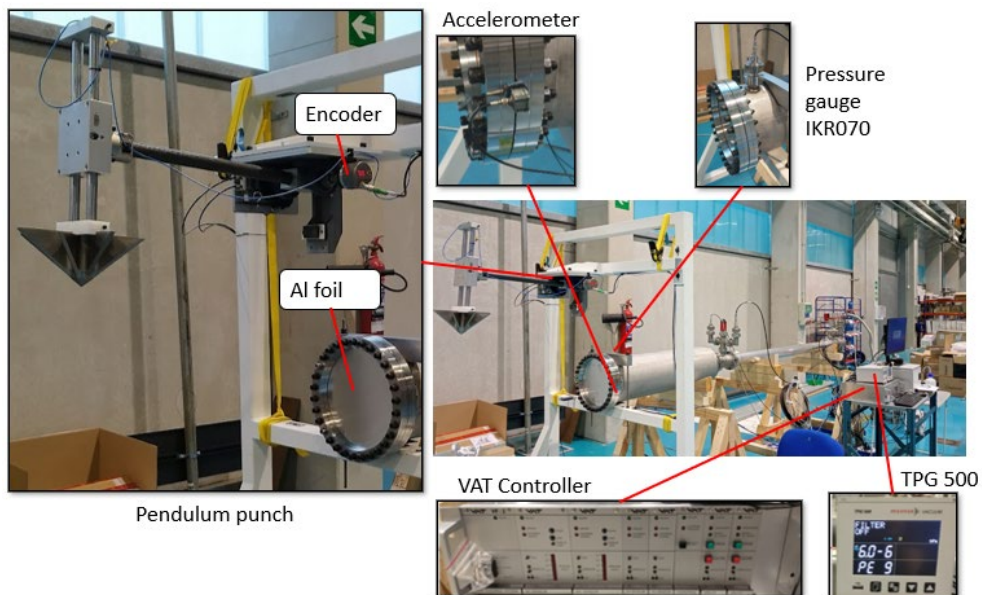
Figure 16. Main components of the P1 prototype.

The Figure 16 shows several images of the setup where some of these experiments were carried out. The prototype P1 setup is composed of the following elements: 3 m long vacuum pipeline + a 1 m/Φ300mm vacuum chamber; one turbomolecular vacuum pump at the end of the line; two IKR070 cold-cathode gauge connected to VAT controller and two Pfeiffer IKR050 cold-cathode gauge connected to a TPG500 controller (Pfeiffer) at the other side of the 3 m line; a punch pendulum with an Al1050 window of 0.5 mm thickness; and a normally open electrical circuit, which on contact between the pendulum and the window closes the circuit allowing detection by means of an analogue signal from the contact.

4.1 Results of the Prototype P1 Tests

Results of test carried out are presented below.

4.1.1 Validation of the Fast Data acquisition of vacuum gauges

For the validation of the response time of the cold-cathode gauges, two different fast DAQ configurations were tested in prototype P1 (Figure 17):

I)   The IKR070 gauges were connected to the VAT FIV Controller. The IKR070 head is provided by Pfeiffer/Inficon, but the sensor controller is integrated in the valve controller. This setup configuration is the one that was used in the CERN experiment [7].

II)   The IKR050 (Pfeiffer/Inficon) gauges were connected to the TPG500 controller provided also by Pfeiffer. It was concluded that the most promising option was to use this TPG500 controller since it has the possibility of disabling all its signal noise filters, which increase considerably the response time. Nevertheless, Pfeiffer informed that there is always a limitation on the response time due to the physical measuring principle of the sensor head itself.

It is worth noting that the IKR050 and IKR070 sensor heads only differ in their sealing solution (the IKR050 has Viton^{TM} seals whereas the IKR070 metal seals). This provides higher the radiation resistance to the later but their operating principles are the same.
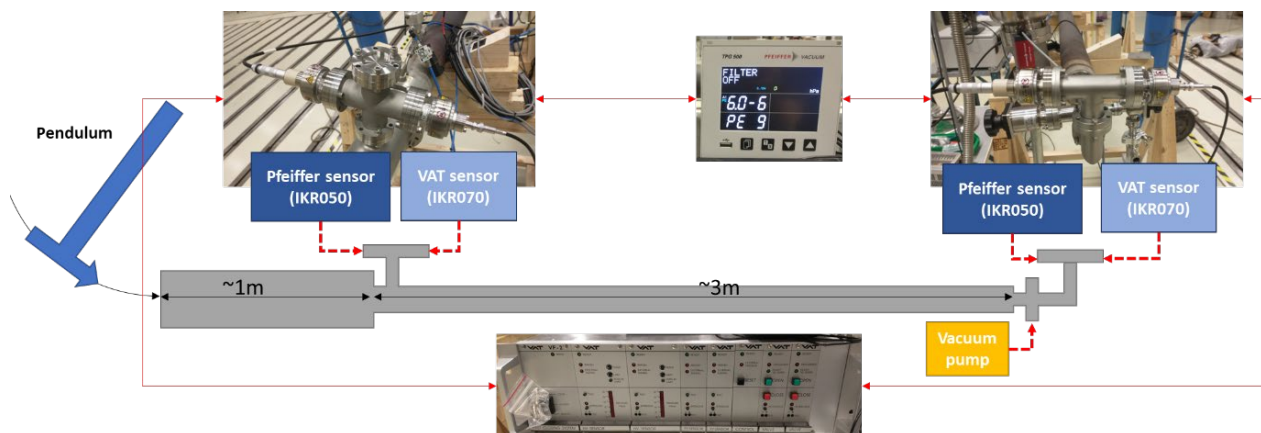
Figure 17. Setup to test two different configurations of the fast pressure gauges acquisition .

Figure 18 shows the results of the tests comparing the response of both sensors and controller configurations when sudden inrushes are generated by the rupture of the aluminium foil. Two main conclusions are obtained. First, the IKR050 with the TPG500 controller (disabling noise filtering stages) detects slightly faster the onset of the pressure rise when the inrush front wave arrives. On the other hand, as shown in the Figure 15, the IKR070 (with VAT controller) has a better time response once the pressure rise starts with a sharper pressure rise which is more consistent with the arrival of the pressure front. Nevertheless, this does not mean necessarily that the IKR070-VAT configuration detects the real stepped pressure rise associated of the front wave, which is probably much faster.
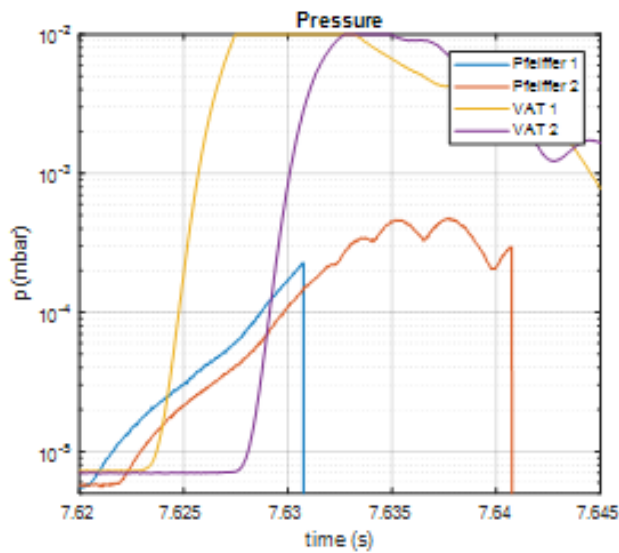
Figure 18. Data recorded form IKR07 gauge pressure. Right, zoom of time response of the gauges.

4.1.2   Validation of the Aluminium Foil Thickness

Different foil thicknesses were tested ranging from 0.2 mm to 0.8 mm. Some images of the broken foils are shown in Figure 19. All the foils were tested dropping the pendulum from the same height and with the same 6-edged cutting tip.

| Al 1050 0.8mm | Al 1050 0.5mm | Al 1050 0.5mm | Al 1050 0.5mm | Al 1050 0.5mm | Al 1050 0.2mm |
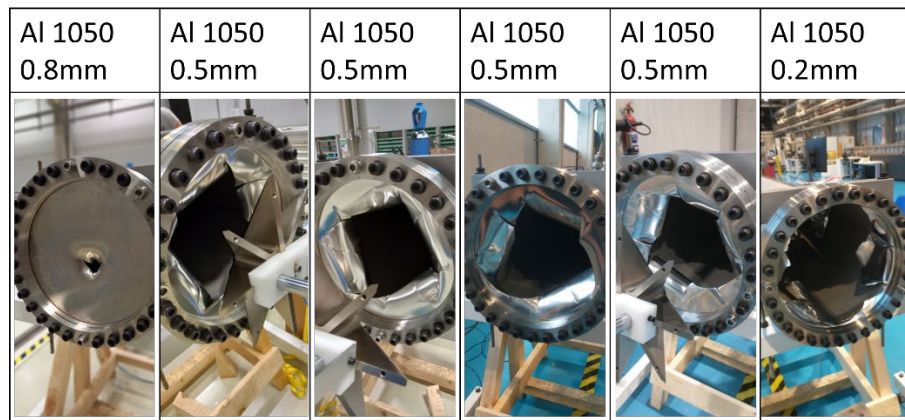
Figure 19. Experimental campaign to evaluate the best thickness for the Al window.

For the case of the 0.8 mm foil, in addition of not having the proper rupture, it was the configuration with which the worst vacuum was obtained, reaching only 10^{-4} mbar. It is believed that it had to do with the sealing mechanism and that the 0.8 mm foil is not ductile enough to deform when tightening the flanges. This is supported by the observation after removing the foil from the test and realizing that a smaller sealing indentation mark with respect to lower thickness foils.

4.1.3   Triggering System for the inrush initialization time

It is critical to know the exact moment in which the air inrush occurs since it allows the determination of the time during which the wave propagates from the air inrush to the sensor. The mechanisms have been studied for this purpose.

Electric Contact: This method works by closing an electrical circuit the punch touches the Al window. This system has been validated and is proven the most accurate one.

Encoder: It consists of an angular encoder attached to the pendulum shaft to acquire its position while falling. Before each test, the angle of contact with the window is established by writing it down manually. This system has been validated but is not as accurate and reliable as the electrical contact.

4.1.4 Estimations of the front wave propagation speed

Finally, the first preliminary results focused on this objective of MuVacAS are presented. The data corresponds to tests carried out with the Prototype P1 setup, shown in Figure 17. The tests consisted in breaking the foil window (0.5 mm thickness) with the pendulum and capturing the pressure rise using the two types of fast pressure acquisition configurations recently introduced. The speed data presented in Table 11 has been estimated based on the comparison of the pressure recording at different sensor positions. Therefore, the eventual intrinsic delay (based on physical measuring principles) of the pressure gauges is not relevant as long as we assume that is the same for all the sensors.

As is shown in the able, propagation speeds up to 720 m/s have been measured, in the order of magnitudes of the values presented in the literature review.

Table 11. Measured front wave propagation speed.

	Tube diameter: Φ300 mm			Tube diameter: Φ100 mm		
TEST DATE	*Sensor configuration*	Initial pressure [mbar]	Relative speed [m/s]	Sensor system	Initial pressure [mbar]	Relative speed [m/s]
06/12/2022	*Pfeiffer*	$5.6\cdot10^{-6}$	640	*VAT*	$7\cdot10^{-6}$	496
07/12/2022	*Pfeiffer*	$4.8\cdot10^{-6}$	658	*VAT*	shut off	-
08/12/2022	*Pfeiffer*	$2.6\cdot10^{-6}$	720	*VAT*	$1.8\cdot10^{-6}$	538
09/12/2022	*VAT*	shut off		*Pfeiffer*	$2\cdot10^{-5}$	519
10/12/2022	*VAT*	$7\cdot10^{-6}$	606	*Pfeiffer*	$1.6\cdot10^{-6}$	510

5. Simulation Activities

In this section a first simulation approach of a sudden air inrush has been developed using CFD to increase the understanding of wavefront propagation in vacuum. When using the Navier Stokes formulation in CFD simulations, the minimum pressure value where the continuous medium hypothesis is fulfilled is 0.1 mbar. For this reason, this pressure is used to represent the vacuum. The ideal gas hypothesis is used, and the gas is considered to be inviscid. Therefore, there is no consideration of the variation of energy terms due to turbulence. The main values for the initial conditions are presented in the Table 12.

Table 12. values for the initial conditions and properties.

Initial Variable and Properties	Value	Units
Vacuum Pressure	0.1	mbar
Atmospheric pressure	1013	mbar
Initial Temperature	300	K
Cp (300K)	1006	J/kg/K
Molecular weight	28.966	mol

5.1 Computational Model

The commercial software ANSYS Fluent is used for the simulation. The geometry proposed for the study has two zones, separated by a "virtual diaphragm": (i) The zone that is at vacuum, representing the dimension of a 250 mm diameter pipe (similar to diameter in the Zone A8, B1, B2 & B3 in MuVacAS). (ii) The zone that is at atmospheric pressure, representing the volume from where the inrush will take place. This is shown in Figure 20. In addition, in order to reduce errors in the continuity equations due to the boundary conditions, a sufficiently large geometry is created in the volume at atmospheric pressure (10 times the diameter of the vacuum line). To reduce the computational calculation, an axisymmetric 2D model is used with an initial quad mesh size of 12.5 mm. In addition, an adaptive meshing is used to re-mesh according to a pressure gradient criterion.
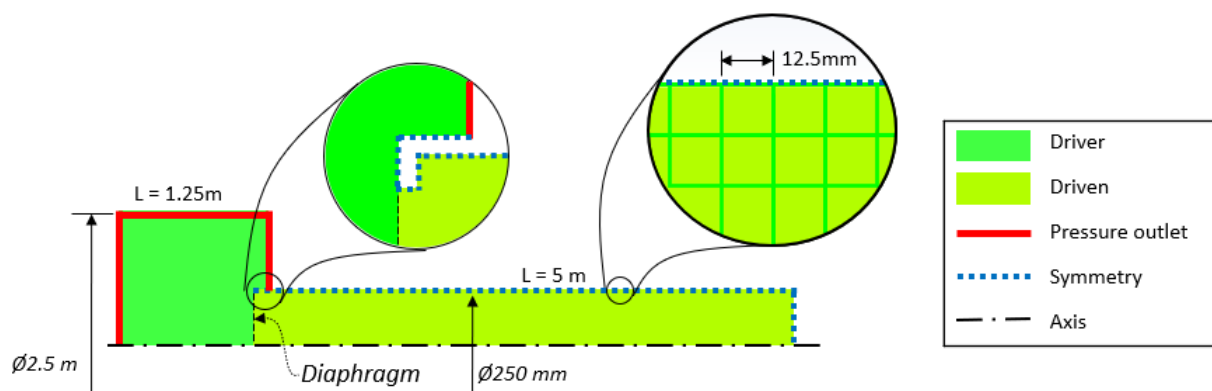

Figure 20. Main characteristics of geometry, meshing and boundary condition.

In addition, the boundary conditions are showed in the Figure 20 and are the following:

- Symmetry, which means an adiabatic condition, also, the normal velocity component, and the normal gradients of all flow variables (viscosity, speed) are thus zero at the symmetry condition.
- Pressure outlet boundary conditions require the specification of a static pressure, it means that all of contour remain to this pressure, in our case is the atmospheric pressure (1013 *mbar*).
- Axisymmetric boundary conditions.

The higher-order ROE - MUSCL scheme is used for the discretization and the default first-order Euler scheme is used for the transient terms. Special treatment is given to the calculation of the time step Δt due to the fact of having waves propagating through a discrete mesh Δx. The time interval must be less than the time necessary for the wave to pass through the adjacent points of the mesh (Courant condition). In addition, it is necessary to control that such condition is always accomplished taking into account that the mesh size changes with each iteration.

5.2 Case Studies

Two case studies have been proposed to understand the dependence of the initial conditions to the inrush propagation speed. The initial values of these two cases are provided in Table 13. In the Case 1, the inrush takes place from a 1 bar atmosphere to 0.1 mbar vacuum. In the Case 2 from a 2 bar atmosphere to 1 bar chamber. It is worth noting that in both cases the pressure difference between the high pressure and low pressure is nearly the same (1 bar). For this reason, the main goal of this comparison is to investigate the differences in the inrushes speed based on the eventual formation of "chocked flow" process, which occurs when inrush velocity is limited by the speed of sound).

Table 13. Values for two different cases of study.

Case	Pressure in the atmosphere [mbar]	Pressure in the line [mbar]	Pressure difference
Case 1	1000	0.1	999.1 mbar (~1000 mbar)
Case 2	2000	1000	1000 mbar

5.3 Results and Discussions

Figure 21 shows the maximum gas velocity over the time for the cases mentioned in the Table 13. The continuous line represents the maximum velocity of the gas in the centre of the tube (axis line) for the case 1, and the discontinuous line represent the same for the case 2.
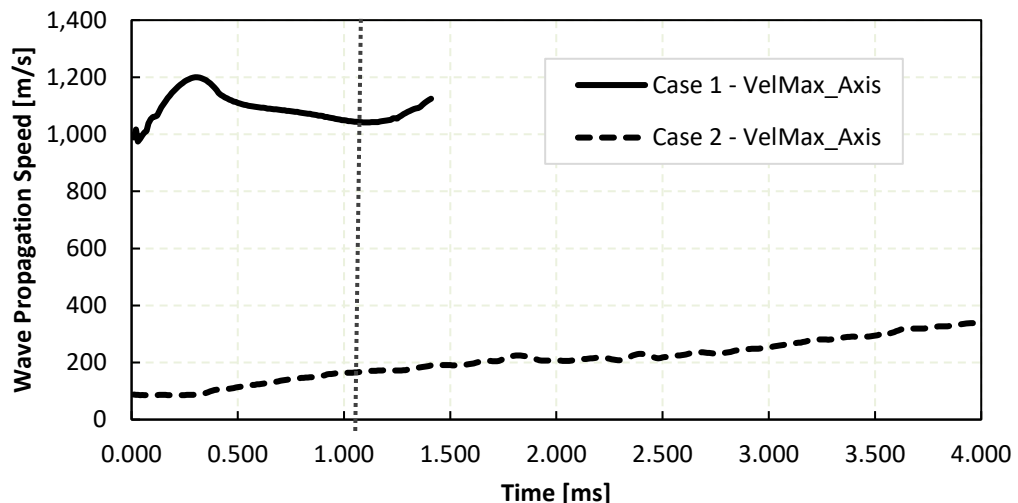
Figure 21. Maximum gas velocity over the time

For the Case 1 (inrush in vacuum) maximum velocities of the order of 1278 m/s are obtained, while for the Case 2, maximum velocities are limited to 480 m/s. To better understand the phenomenon, a map of velocities at 1 ms after the rupture for the two cases is presented in Figure 22.
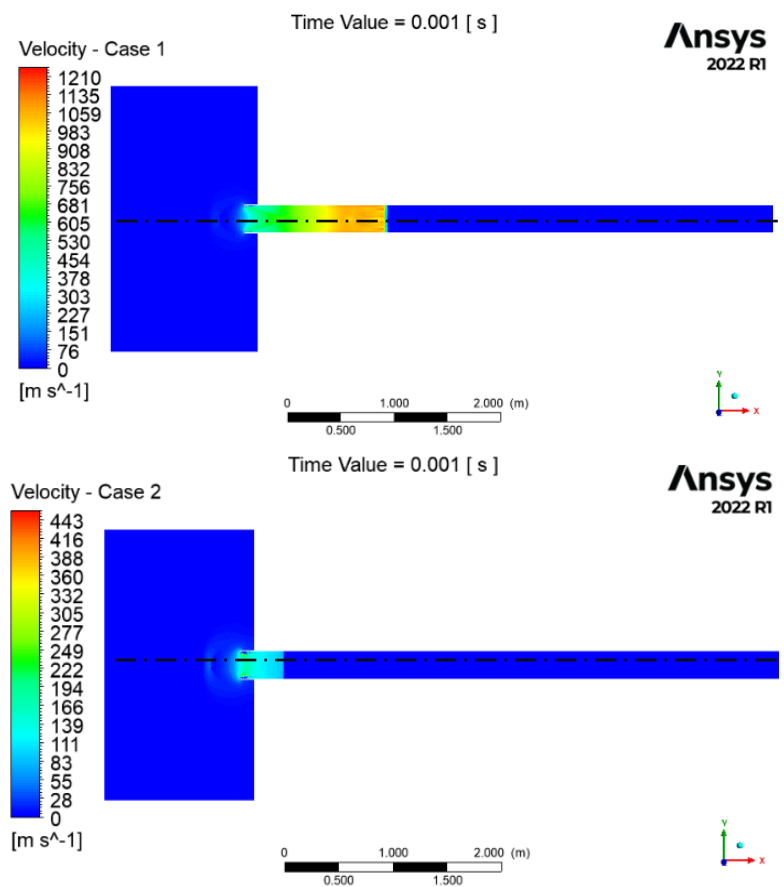

Figure 22. Velocity profile for the wave front propagation in the cases 1 & 2, to t = 1 ms.

Table 11 compares the obtained results of the vacuum case with the Riemann models, better known as the Shock Tube Problem (STP) and the analysis described by Takiya et al. [5] for the propagation of shock waves in vacuum, leading to a difference of lower than 8.7 % in the predictions.

Table 14. Wavefront velocity comparison between the analytical models with the simulation results, Case 1.

| Variable	Value	Unit
Pipe internal Diameter (D)	0.250	*m*
Air Diameter d	0.225	*m*
Betha (d/D)	0.9	
Max. Vel. by Tayika **[5]**	1400	*m/s*
Shock Tube Problem	1318	*m/s*
Max. Vel. ANSYS	1278	*m/s*
Relative error_ Tayika	**8.7**	%
Relative error_ STP	**3.1**	%
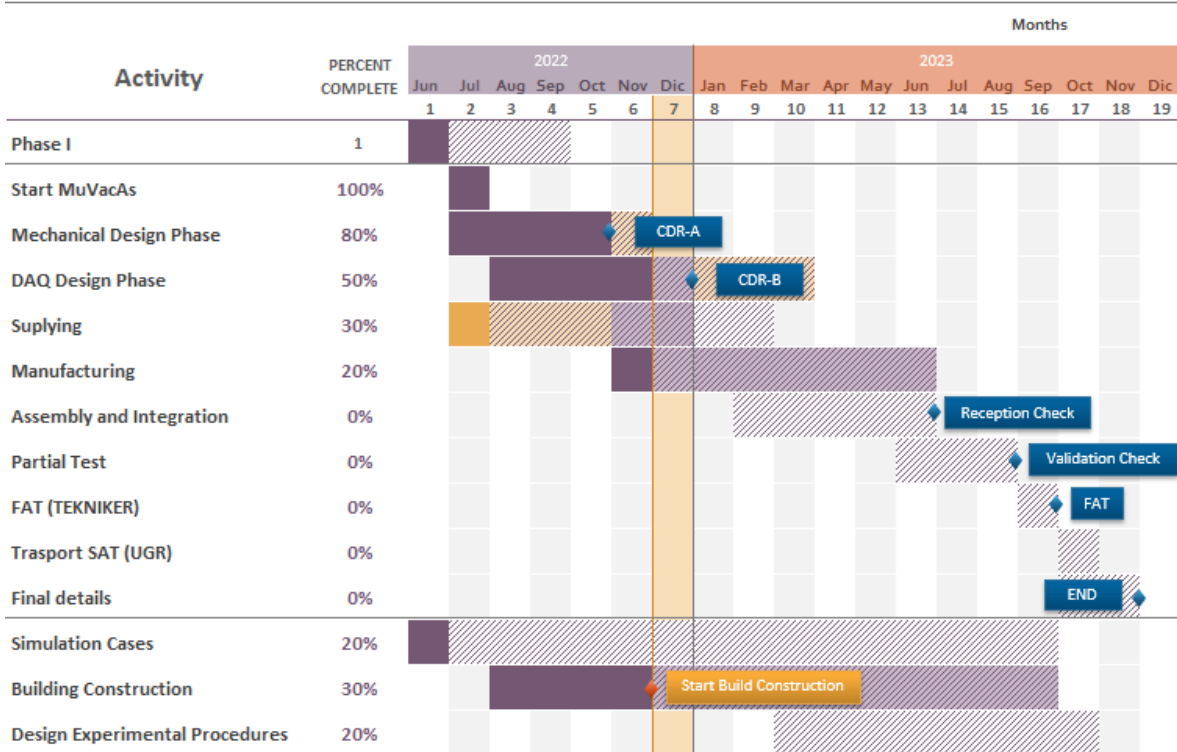
This type of simulations allows the characterization of pressure, temperature, density and gas energy along the time and the domain. This will be very useful for the understanding of the phenomena and results interpretation during experimental campaigns. Future simulations will aim at reproducing conditions closer to reality. For instance, with an eventual time variation of the geometry (diaphragm) to recreate the rupture of the foil. This aspect may be quite relevant since the time range in which the rupture occurs is the same order of magnitude of the time response of the wavefront velocity in this geometry (Ø250 mm).

6. Conclusions and Next Steps

This report provided an overview of the technical design of the MuVacAS Experimental Setup. First prototyping activities have validated the design of the Fast Data Acquisition system, the aluminium foil thickness, and the triggering system for the inrush onset. For the Fast Data Acquisition system, it has been selected a set of the IKR050 pressure gauge connected analogically with the TPG500 controller, which will have an input signal to the NI-DAQ acquiring at kHz. For the recreation of the back plate rupture, it is known that the 0.3 mm and 0.5 mm thick foils have the best rupture and repeatability. A 0.2 mm foil could be also used, provided that additional action must be taken to prevent the access of foil debris to the pumping units and that it can be easily removed after each experiment.

Front wave propagation speed of air inrushes in vacuum have been estimated by using the relative measurement of pressure sensors, obtaining a maximum value of 720 m/s for an initial vacuum of $2.6 \cdot 10^{-6}$ mbar. Complementary to this activity, CFD simulations have estimated a propagation velocity reaching values of 1200 m/s. This 43% discrepancies are attributed to the strong assumptions of the modelling (such as instantaneous rupture) among others. Thes preliminary models and measurements will be investigated further during the experimental campaigns. The activities presented in Table 15 have been carried out at satisfactory progress rate and is estimated that MuVacAS will be operational by Q4 of 2023.

Table 15. 2023 Schedule for MuVacAS in 2023.

Months

| Activity	PERCENT COMPLETE	2022							2023												
		Jun	Jul	Aug	Sep	Oct	Nov	Dic	Jan	Feb	Mar	Apr	May	Jun	Jul	Aug	Sep	Oct	Nov	Dic
		1	2	3	4	5	6	7	8	9	10	11	12	13	14	15	16	17	18	19
Phase I	1																			
Start MuVacAs	100%																			
Mechanical Design Phase	80%						CDR-A													
DAQ Design Phase	50%							CDR-B												
Suplying	30%																			
Manufacturing	20%																			
Assembly and Integration	0%														Reception Check					
Partial Test	0%																Validation Check			
FAT (TEKNIKER)	0%																FAT			
Trasport SAT (UGR)	0%																			
Final details	0%																	END		
Simulation Cases	20%																			
Building Construction	30%							Start Build Construction												
Design Experimental Procedures	20%																			

7. References

[1] "Safety Analysis Report 2.0," EFDA_D_2PN9XX, 2022.

[2] C. Torregrosa, "ENS-6.1.4.0-T001-03-N1_Design of an experiment to test vacuum-related accidents," IDM: (2PE6K4 v1.0)..

[3] H. Betz, A. Heuberger and P. Hofbauer, "Measurements on the efficiency of acoustic delay lines in view of beam lines for synchrotron radiation," *Journal of Vacuum Science and Technology,* vol. 16, no. 3, p. 1979, 924.

[4] W. Peatman and E. W. Weiner, "Measurements of shock wave flight times in long pipes," *Journal of Vacuum Science and Technology,* vol. 17, no. 5, pp. 1237-1240, 1980.

[5] T. Takiya, F. Higashino and M. Ando, "Pressure wave propagation by gas expansion in a high vacuum tube," *Journal of Vacuum Science & Technology,* vol. 17, pp. 2059-2053, 1999.

[6] M. Ady, "Measurement campaign of 21-25 July 2014 for evaluation of the HIE-ISOLDE inrush protection system," CERN EDMS 1414574, Geneva, 2014.

[7] M. Ady, M. Hermann, R. Kersevan, G. Vandoni and D. Ziemianski, "M. Ady, M. Hermann, R. Kersevan, G. Vandoni and D. Ziemianski,," in *Proceedings IPAC*, 2014.

[8] M. Otawa and T. Kunugi, "Thermohydraulic experiments on a water jet into vacuum during ingress of coolant event in a fusion experimental reactor," *Fusion Engineering and Design,* vol. 29, pp. 233-237, 1995.

[9] N. Garceau, . S. Bao, W. Guo and S. Van Sciver, "The design and testing of a liquid helium cooled tube system for simulating sudden vacuum loss in particle accelerators," *Cryogenics,* vol. 100, pp. 92-96, 2019.

[10] P. Anger, V. Cingal, J. C. Pacary, S. Perret-Gatel and A. Savalle, "SAFETY SYSTEM FOR THE RESPECT OF NUCLEAR REQUIREMENTS OF SPIRAL2 FACILITY," in *Proceedings of IPAC2020*, 2020.

[11] E. Blanco Vinuela, B. Fernandez Adiego, R. Speroni and S. F. Braunmueller, "Safety Instrumented Systems and the AWAKE Plasma Control as a Use Case," in *ICALEPCS2017-THCPA01*, 2017.

[12] V. Petwal and et al, "Interlock system with fast response against sudden foil rupture and vacuum failure in Linac structure," 2013.

[13] M. Dommach, M. Di Felice, B. Dickert, J. Eidam, N. Kohlstrunk and R. Villanueva, "The photon beamline vacuum system of the European XFEL," *Journal of Synchrotron Radiation,* vol. 28, no. 4, pp. 1229-1236, 2021.

[14] M. S. Ferreira, "Fast response of cold-cathode and ion pumps for interlock system," NSLS II Vacuum Group, 2011.

[15] "CAD - 06.06_HEBT and Beam Dump 3D Mock-up (2MVLX3 v5.1)," EFDA_D_2MVLX3, 2022.

[16] "CAD - 05.02_Target_System_2MQ99Q_v1_1," EFDA_D_2MQ99Q, 2021.

[17] "TID-6.6.1-23-01 Modifications last section of HEBT for optimization of interfaces," EFDA_D_2PNEYN, v2.0, 2021.

[18] "ENS-6.6.1.0-T25-09-R1 HEBT Final Engineering Design Report 2020," EFDA_D_2NNS3E, 2020.

[19] VAT, "VAT Catalogue FIV Series 75.0," [Online]. Available: https://www.vatvalve.com/series/ultra-high-vacuum-fast-closing-valve-flap-valve-version. [Accessed 2021].

[20] R. C. Dhuley, Gas propagation in a liquid helium cooled vacuum tube following a sudden vacuum loss, The Florida State University, 2016.

[21] V. Hauer and C. Day, "Vacuum modelling of the IFMIF-DONES vacuum system," ENS-6.1.4.0-T29-01-N1, 2021.

8. Appendix 1: Time-line of the Literature Review.

TIME-LINE BIBLIOGRAPHY

9. Appendix 2: Diagram of MuVacAS